Ecole Polytechnique
Fédérale de Lausanne

Urban thermodynamics

Course Project 2024 : Case study - EPFL Innovation Park

Auteurs

Malika Jenni, SCIPER : 298980
Alexia Goumaz, SCIPER : 341128
Alexandra Van Oost, SCIPER : 344983
Emilie Scascighini, SCIPER : 346219
Cyril Bonny, SCIPER : 324490
Loïc Antille, SCIPER : 346325

Report Group 2

January 9, 2025

Prof. Dolaana Khovalyg, Kun Lyu

CIVIL-309
Autumn semester - 2024

Table of contents

1 Introduction

As cities continue to expand and densify, urban overheating presents significant challenges to sustainability and livability. Urban heat islands (UHIs), a pressing issue in urban design, amplify the impacts of global warming and urban growth, leading to thermal discomfort, increased energy demand, and public health risks. Urban heat islands result from factors such as extensive use of heat-retaining materials, reduced vegetation cover, and anthropogenic heat emissions. Addressing this issue requires a comprehensive understanding of how urban elements influence microclimates and thermal energy dynamics.

Located near Lake Léman and characterized by diverse ground materials, the EPFL Innovation Park offers an ideal setting to study and mitigate the effects of urban overheating. The objective of this project is to examine the influence of urban elements on the urban microclimate and thermal energy exchange, investigate their interactions, and explore strategies to mitigate urban overheating.

First, we will analyze the current conditions of the site, including aspects such as Local Climate Zone (LCZ), material properties, urban morphological parameters, green elements, and climatic characteristics, to better understand its microclimate.

Next, we will evaluate specific aspects of buildings, ground cover, vegetation, and water features to understand their effects on the urban microclimate and propose improvements in response to continuous urban growth and emerging challenges.

Finally, we will integrate the effects of multiple urban elements on energy exchange and the microclimate. Based on this analysis, we will propose an optimized intervention strategy to enhance the site's future climatic conditions and better prepare it to address the challenges urban environments will face. This project aims to deliver actionable insights for creating more resilient and sustainable urban designs.

Central to this work is the use of ENVI-met to model thermodynamic interactions and assess intervention impacts. Using future climate scenarios for 2100, the project incorporates advanced analytical techniques to address the long-term challenges posed by climate change.

Figure 1: Overview Site : EPFL Innovation Park.

2 Site analysis

2.1 General Introduction

The EPFL Innovation Park, located in the southwest part of the EPFL campus near Lake Geneva, serves as a dynamic hub for innovation and technological advancement. It was established as a community for start-ups, scale-ups, research units, and established technology firms, fostering collaboration and development in cutting-edge fields.

The site covers an area of approximately 11 hectares and features a mix of rectilinear office buildings, a parking lot, and an urban woodland, bordered by roads on three sides. It is adjacent to residential areas to its west and south, making it an integrated yet distinct part of the local urban fabric.
The road network around the site provides efficient connectivity, supporting its role as a center for professional and academic activities.

Internally, the site is characterized by four types of ground cover materials: asphalt roads, sandy soil, cement concrete pavement, and loam soil, which influence its thermal properties and interaction with the local microclimate.

Next, we have 3 types of buildings. The composition of the facades and roofs of each type of building is presented in Table 1.

Category	Layer	**Building Group A**		**Building Group B**		**Building Group C**	
		Material	Thickness [m]	Material	Thickness [m]	Material	Thickness [m]
Facade	1	Prefabricated concrete wall	0.14	Plaster	0.01	Fiber cement board	0.008
	2	Insulation	0.1	EPS Expanded Polystyrene	0.18	Sandwich panel mineral wool	0.15
	3	Plaster	0.047	Plywood (heavyweight)	0.14	Aluminium	0.002
Roof	1	Gravel	0.05	Gravel	0.1	Gravel	0.04
	2	Insulation	0.2	XPS Extruded polystyrene CO2 blow	0.2	Mineral wool insulation	0.08
	3	Reinforced concrete slab	0.3	Concrete reinforced with 2% steel	0.3	Reinforced concrete slab	0.35
	4	-	-	EPS Expanded Polystyrene	0.065	-	-

Table 1: Building facade and roof materials.

Figure 2: Base Case - Site Creation in ENVI-met.

Legend: vegetation (green), buildinds (gray).

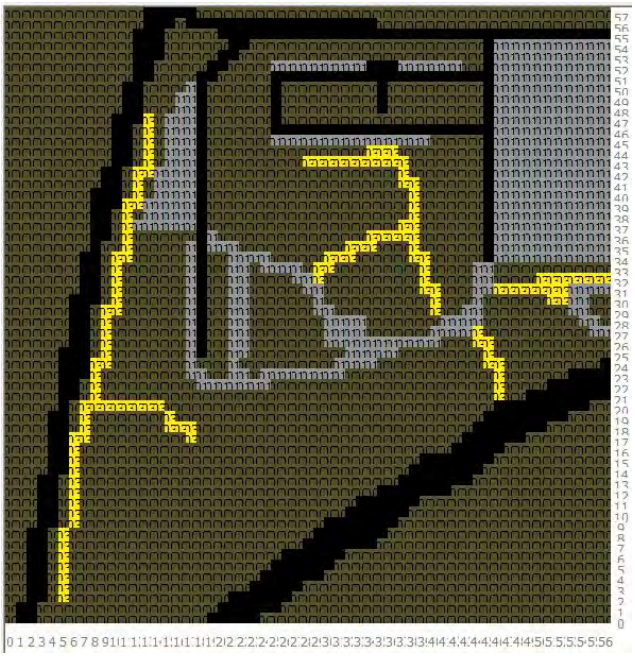

Figure 3: Base Case - Site Soil Creation in ENVI-met.

Legend: asphalt (black), cement concrete (gray), sandy (yellow), sandy loam (green-brawn).

2.2 Climate Analysis

The Climate Analysis of the epw weather data given of the Esplanade was done on the website CBE Clima Tool.

The provided data describes a future climate scenario for the Esplanade, near the EPFL Innovation Park, located at latitude 46.52° N, longitude 6.566° E, and an elevation of 398 m. Based on the data there are moderate temperature variations with no extreme seasonal dryness.
Here is a more detailed analysis:

1. Temperature Profile:

   - Average yearly temperature: 16.1 °C, indicating a mild climate throughout the year.
   - Hottest temperature: 39.4 °C, suggesting occasional heatwaves, particularly in summer.
   - Coldest temperature: -1.4 °C, implying that freezing conditions are rare and winters are relatively mild.

2. Solar Radiation:

   - Annual cumulative horizontal solar radiation: 1420.38 kWh/m^2, reflecting moderate solar exposure.
   - Diffuse horizontal solar radiation: 39.1%, showing a significant proportion of indirect sunlight due to atmospheric conditions, such as cloud cover or haze.

The hottest day of the year is July 21, with potential temperatures reaching up to 39.40 °C according to the CBE Clima Tool. Relative humidity ranges from 17 to 24 g/kg. Wind speeds vary up to 1.3 m/s. A few millimeters of precipitation occur between 6:00 PM and 8:00 PM.
However, due to excessive wind variation, we will conduct simulations for August 18, which is also one of the hottest days.

3. Climatic Implications:

The results indicate consistent precipitation, moderate humidity, and a stable annual temperature range, minimizing thermal stress and supporting diverse ecosystems. Moderate solar radiation suggests potential for solar energy projects, though frequent overcast conditions may reduce efficiency. An average temperature of 16.1 °C, significantly higher than historical Cfb norms, points to potential climate change effects, likely impacting vegetation, water resources, and building design strategies.

To conclude, the site analysis' climate is mild with moderate potential for solar energy and relatively stable weather patterns. The warming trend indicated by the future data warrants adaptive measures to mitigate potential risks, such as heatwaves and increased energy demands.

2.3 Thermal Properties of Urban Surface Materials

The building façades are primarily composed of materials such as concrete, plaster, and fiber cement boards. These materials, with moderate thermal conductivity and high thermal mass, tend to absorb and store heat during the day, releasing it slowly at night, which can contribute to localized warming. The roofs are covered with gravel, a material with relatively low albedo (0.2–0.3), which absorbs solar radiation but also provides some reflective capacity depending on its color and texture.

Ground surfaces consist of asphalt roads, sandy soil, cement concrete pavement, and loam soil. Asphalt, with its low albedo (0.05–0.2) and high thermal storage, contributes significantly to daytime heating. Cement concrete surfaces reflect more sunlight (0.3–0.5) but can also retain heat, depending on their texture and composition. Sandy and loam soils offer natural cooling potential due to their lower thermal storage and capacity for moisture retention, which enhances evapotranspiration effects.

In contrast, grass and trees provide cooling effects through shading and evapotranspiration, mitigating heat buildup. These thermal properties influence surface temperatures and contribute to local variations, especially in open or shaded areas.

These material properties, combined with the area's urban morphology, influence the surface temperatures and contribute to the site's microclimate dynamics, and will help us understanding and finding critical hotspots.

2.4 Neighbourhood characteristics

The project started with a site visit. During this visit, we estimated parameters related to natural elements, ground cover materials, surrounding building materials, surrounding building heights, anthropogenic heat sources, aspect ratio, sky view factor, and shading resources at several locations.

You will find the table we filled out during this visit in the appendix (Figure 83).

These data provided us with an initial understanding of the site, including the materials used for the buildings and the ground. Regarding vegetation, we identified the density of trees and bushes in certain areas with greater precision. We observed that the majority of the site is covered with grass, with scattered trees here and there, and bushes spread throughout the area. As for the ground cover materials, we found that they were mostly either asphalt or gravel. Additionally, we estimated the heights of some buildings: 22 meters for some, 13 meters for others, and two at 14 meters. We also observed that the buildings are spaced at varying distances from each other, with some having more considerable gaps between them, indicating that the building density is relatively low. Based on these observations, we classify the site as a Local Climate Zone LCZ 5, open midrise.
This classification suggests that the site has a moderate impact on the local surface climate. The relatively low building density, combined with the presence of vegetation and open spaces, allows for some ventilation and heat dissipation, though impermeable surfaces like asphalt and gravel may contribute to localized warming.

Regarding the buildings' composition, we found that they are predominantly made of metal, concrete, and glass. All of these observations are well supported by the actual materials of the ground and buildings, we mentioned earlier.

The trees and buildings also serve as important shading resources, helping to reduce solar radiation in certain areas of the site.
For specific locations, we calculated the aspect ratio to evaluate the risk of canyon formation, using the formula : $\lambda_s = \frac{H}{W}$, where H is the height of the building, and W is the width of the potential canyon.

For each location, we also estimated the sky view factor. To do this, we used the „FishEyeVideo" application, which captures the landscape through a lens similar to that of a door viewer. Figure 4 and figure 5 present two examples of the estimated sky view factor.

Figure 4: $\psi_{sky} = 1$ (Location 1).

Figure 5: $\psi_{sky} \approx 0.75$ (Location E).

2.5 Simulation for Base Case

We first conducted a Base Case simulation using ENVI-met.
Initially, we created the site model on 'Spaces,' using materials that were matched as closely as possible to those specified in the project description. If the required materials were not already available, we created new ones in 'Spaces'. The thermal properties used were obtained from the Ubakus website provided in the course. Any missing information was sourced using ChatGPT.

Once the model was completed, we ran an initial simulation of the site's conditions for the year 2100.
All the simulations were made for the day of August 18.
According to the EPW data, this day has potential temperatures ranging from 30 to 40°C, which is very hot. The relative humidity ranges from 19.5 to 23.5 g/kg. The shortwave direct radiation peaks significantly between 6 AM and 8 PM, reaching almost 800 W/m^2. There is a light breeze in the morning from 6 to 8 AM, with a maximum speed of 2.8 m/s. There is no precipitation during this day.

The results were then analyzed using 'Leonardo' and are detailed below.
A height of k=2 (= 2.5m) was chosen for the simulation analysis, in order to represent the standard measurement height for air temperature and humidity, as well as to align with the typical height at which human thermal comfort is evaluated.

2.5 meter height is generally not used to assess pedestrian thermal comfort (it is too high for human).

2.5.1 Air Temperature

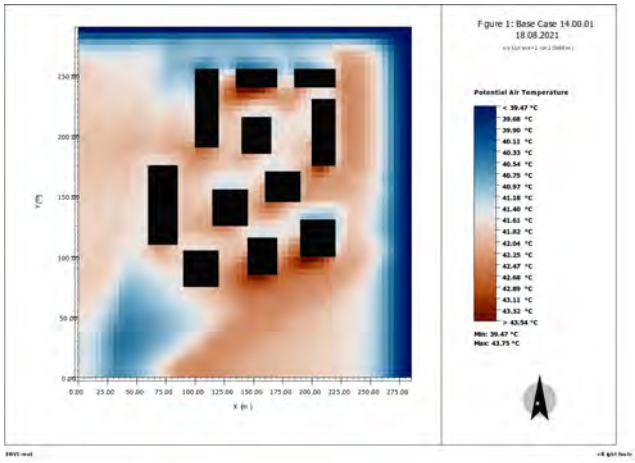

Figure 6: Base Case-Potential Air Temperature 2 PM.

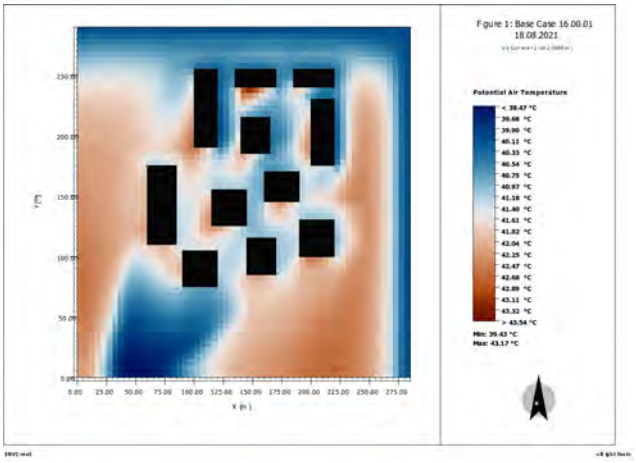

Figure 7: Base Case-Potential Air Temperature 4 PM.

In the simulation of the potential air temperature distribution of the site, distinct temperature variations can be observed depending on the location. The temperature values range from 39.47°C to 43.75°C at 2PM, and from 39.43°C to 43.17°C at 4PM.

Blue areas correspond to lower temperatures, whereas reddish-brown zones indicate higher temperatures. The cooler blue area is located behind the forest in the bottom-left corner, confirming that vegetation reduces surrounding temperatures through evapotranspiration and shading effects. In contrast, the warmer zones are concentrated near buildings, likely creating heat islands due to the heat-retaining properties of construction materials.
The hottest area is located in the top-right corner, where the surface is dominated by a large parking lot covered with asphalt, a material known for its high heat absorption and retention.

Based on these observations, we conclude that incorporating vegetation is an effective strategy for mitigating urban heat and achieving a more balanced thermal environment.

What is also interesting to note here is that after 2 PM, the temperatures drop a little bit between the buildings, likely due to increased shading in the afternoon, while the areas exposed directly to the sun remain at about the same temperature.

2.5.2 Relative Humidity

This simulation represents the distribution of relative humidity across the site, with values ranging from 39.53% to 48.59%. Areas with lower humidity are shown in reddish-brown tones, while higher humidity zones are in blue.
The highest relative humidity levels are located in the bottom-left corner, where vegetation is present. This confirms that vegetation increases surrounding humidity through evapotranspiration, as plants release moisture into the air. The lowest humidity levels are observed in the top-right corner, which is dominated by a parking lot covered with asphalt. Asphalt surfaces do not retain or release moisture, leading to drier local conditions.
The buildings also appear to contribute to localized reductions in humidity due to the absence of vegetation and the heat radiated from their surfaces, which can dry out the surrounding air.
Between the green areas and built-up zones, there is a gradual transition in humidity levels, illustrating the influence of vegetation on the microclimate.

This highlights the importance of vegetation in regulating humidity and it confirms that integrating green infrastructure into urban environments can help mitigate the effects of drier conditions caused by impermeable surfaces and buildings.

2.5.3 Surface Temperature

This simulation represents the surface temperature distribution across the site, with values ranging from 25.80°C to 59.82°C. Areas with lower temperatures are shown in blue, while higher temperatures are depicted in reddish-brown.
The coolest areas are found in the bottom-left corner, where vegetation is present. This confirms the cooling effect of green spaces, which lower surface temperatures through shading and evapotranspiration. On the other hand, the hottest areas are located in the top-right corner, corresponding to a large asphalt parking lot. Asphalt retains and radiates heat, resulting in significantly higher surface temperatures.
The buildings do not display temperature values but likely contribute to localized heat increases due to the thermal mass effect of surrounding materials.
A noticeable temperature gradient can be observed between vegetated zones and impervious surfaces, illustrating how surface types influence urban thermal conditions.
This analysis highlights the importance of incorporating vegetation and selecting appropriate surface materials to mitigate heat in urban environments.

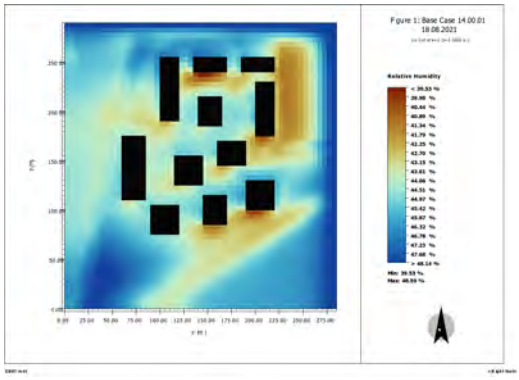

Figure 8: Base Case - Relative Humidity.

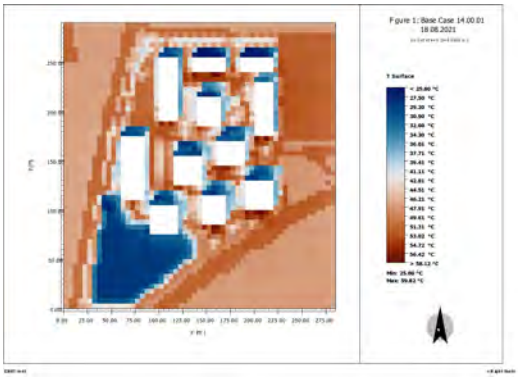

Figure 9: Base Case - Surface Temperature.

Figure 10: Base Case-3D Visualisation.

2.5.4 Wind

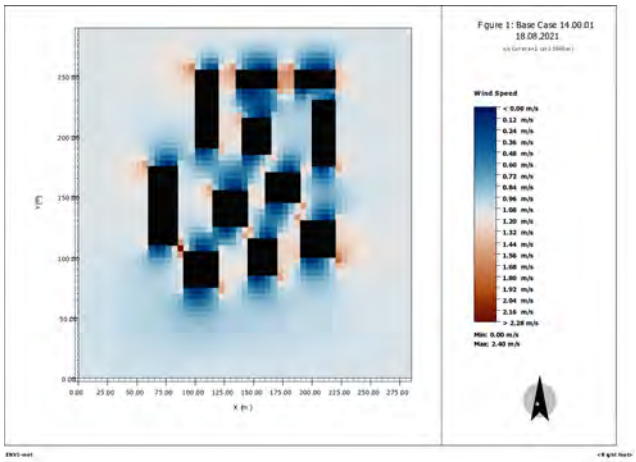

Figure 11: Base Case - Wind Speed.

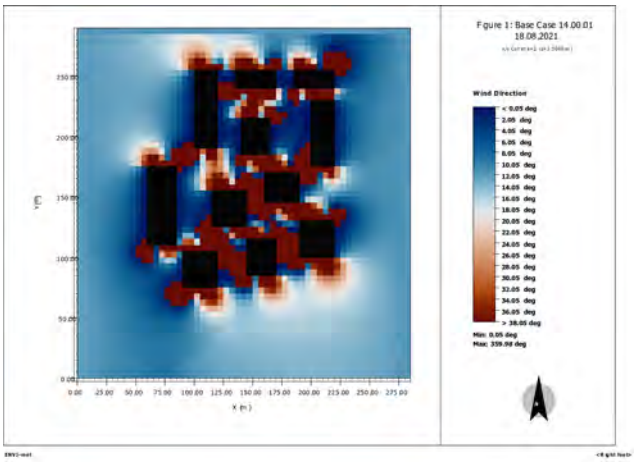

Figure 12: Base Case - Wind Direction.

The simulation shows wind flow patterns across the site, with wind speeds ranging from 0.00 m/s to 2.40 m/s. Variations in wind behavior are influenced by the layout of buildings and vegetation.

In the bottom-left corner, the vegetated area allows for higher wind speeds and smoother flow, as there are fewer obstructions. This contributes to cooling in this zone, supporting the idea that vegetation enhances ventilation and reduces heat.

In contrast, near the buildings, especially in the central and upper-right areas, wind flow is reduced and becomes more turbulent. The buildings act as barriers, slowing the wind and trapping heat. This creates stagnant zones with limited airflow, which contributes to the urban heat island effect.

The simulation highlights how urban design significantly influences wind behavior, with vegetation promoting cooling and airflow, while dense structures hinder it.

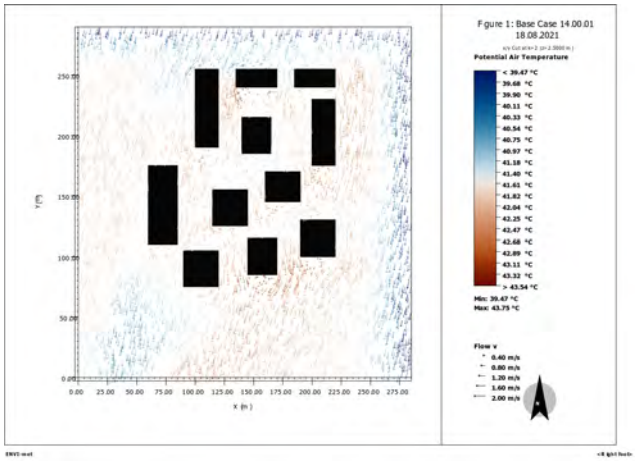

Figure 13: Base Case - Wind Vectors.

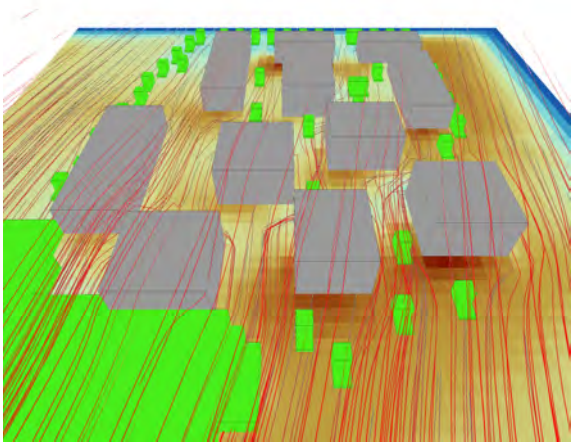

Figure 14: Base Case - 3D Wind Map.

2.5.5 Radiation

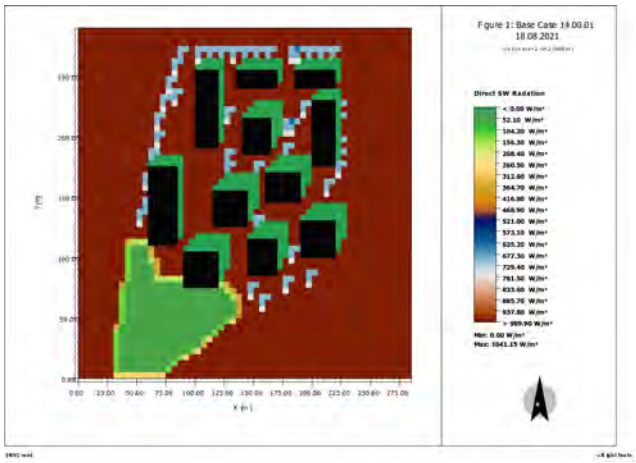

Figure 15: Base Case - SW Direct Radiation.

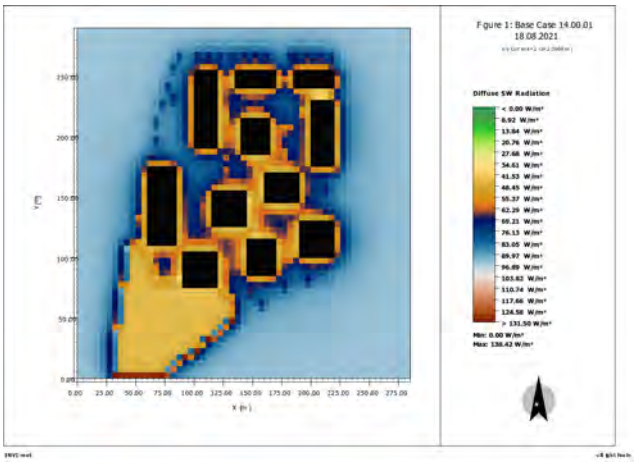

Figure 16: Base Case - SW Diffuse Radiation.

These four figures illustrate the distribution of direct shortwave (SW) radiation, diffuse shortwave radiation, and longwave (LW) radiation from the upper and lower hemispheres, respectively.

Figure 15 shows the distribution of direct SW radiation, with the scale ranging from areas with minimal exposure ($<$0.00 W/m^2, shown in green) to zones with the highest exposure (up to 1041.15 W/m^2, in brown). Blue and green areas, which are primarily shaded regions behind buildings or under trees, receive little to no direct sunlight, helping to limit local heat gain. Conversely, brown zones, typically found in open spaces, represent areas of maximum exposure, significantly contributing to the urban heat island effect.

Figure 16 illustrates the diffuse SW radiation, which is more uniformly distributed compared to direct radiation. The scale ranges from $<$0.00 W/m^2 (in green) to 138.42 W/m^2 (in brown). Yellow and orange areas indicate moderate exposure due to scattered solar radiation, often seen in semi-open or less shaded areas.

Figure 17 presents the LW radiation emitted from the upper hemisphere. The scale ranges from $<$413.09 W/m^2 (in green) to 556.29 W/m^2 (in brown). Areas with high LW radiation levels (brown and orange zones) typically correspond to surfaces that absorb and re-emit significant amounts of heat, often near buildings or hardscapes.

Finally, figure 18 shows the LW radiation emitted from the lower hemisphere. The scale ranges from $<$468.72 W/m^2 (in green) to 676.22 W/m^2 (in brown). This figure captures the radiation emitted from ground-level surfaces. The green zones, particularly in areas covered by vegetation, demonstrate the cooling effects of natural elements. On the other hand, brown and orange regions, typically located near building foundations or hardscapes, indicate higher emissions due to absorbed heat, further contributing to the urban heat effect.

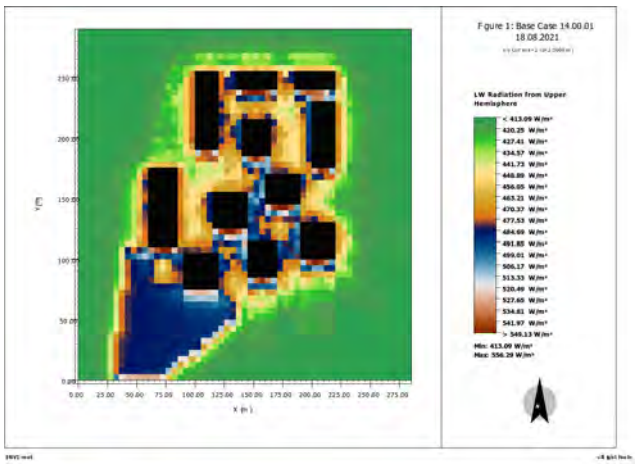

Figure 17: BC - LW Radiation Upper Hemisphere.

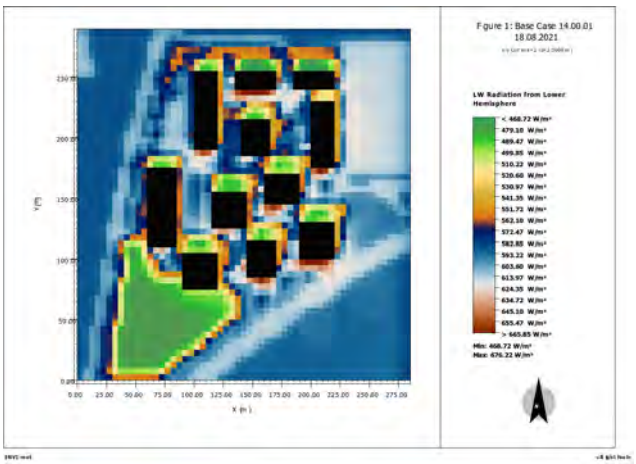

Figure 18: BC - LW Radiation Lower Hemisphere.

2.6 Thermal Comfort

For the thermal comfort analysis, we simulated the Universal Thermal Climate Index (UTCI) for a default female with summer clothing using BIO-met.

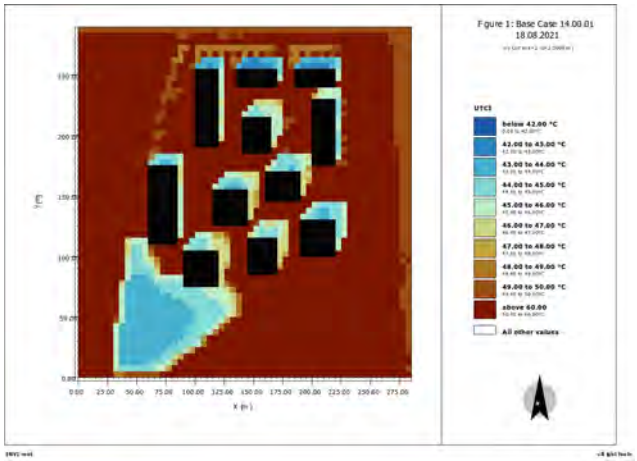

Figure 19: Base Case - UTCI.

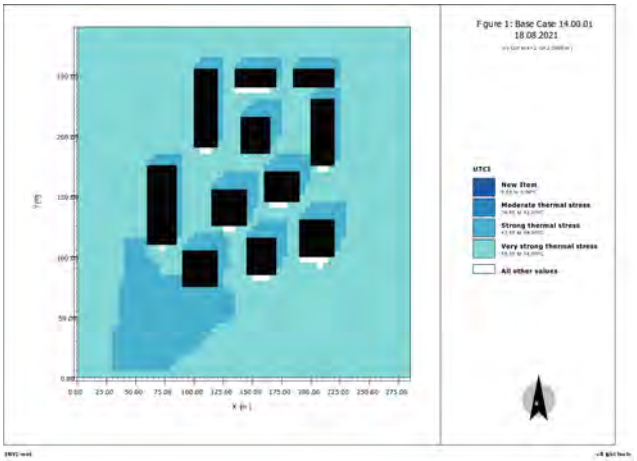

Figure 20: Base Case - Thermal Stress (UTCI).

The map on the left shows UTCI temperature ranges, variations going from "below 42°C" to "above 60°C." Cooler zones in blue are near shaded areas, while open spaces show higher temperatures in red and brown. This visualization highlights zones with significant heat exposure, underlining the importance of shading and vegetation in mitigating urban heat effects.

The map on the right shows a discrete categorization of the UTCI into Thermal Stress categories. The distribution of UTCI values reveals distinct patterns influenced by shading and solar exposure. Areas experiencing Moderate Thermal Stress (36°C to 42°C) are primarily located near shaded zones, such as the northern sides of buildings or areas influenced by vegetation. These zones show reduced thermal stress due to decreased exposure to direct solar radiation.

In contrast, Strong Thermal Stress (42°C to 48°C) is observed in open spaces exposed to direct sunlight, where shading is minimal or absent. These regions are likely dominated by heat-retentive surfaces such as asphalt or concrete, intensifying thermal discomfort.

Furthermore, areas with Very Strong Thermal Stress (48°C to 56°C), represented blue-green, are concentrated in large open spaces between buildings.

This emphasizes the significant impact of urban surface materials and direct solar exposure on thermal comfort.

The buildings influence surrounding thermal stress levels by casting shadows. Shaded areas near buildings generally exhibit lower UTCI values, highlighting the positive effect of shading in mitigating thermal discomfort. The orientation of buildings and the time of day also play a important role in determining thermal stress levels. Southeastern zones, for instance, appear more exposed to direct sunlight, leading to higher stress levels.

From an urban planning perspective, these results underline the importance of integrating shading and heat mitigation strategies to improve thermal comfort. High-stress areas would benefit from additional green infrastructure, such as trees or green walls, to provide natural shading and cooling effects. Moreover, replacing heat-retentive surfaces with reflective or permeable materials could reduce ground-level temperatures. The orientation of future buildings should also consider maximizing shading during peak sunlight hours.

3 Urban microclimate exploration

3.1 Building environment interactions

This section addresses the interaction between buildings and the environment. We will therefore aim to understand the impact of urban morphology.

3.1.1 Modifications for second simulation

We decided to modify the urban morphology to enhance the comfort of people within the Innovation Park. It is well known that when buildings are too tall, there is a risk of wind gusts forming between them due to several factors.
First, there is the channeling effect: tall buildings create a phenomenon called the Venturi effect, where wind speeds up as it passes between two closely spaced structures. By reducing the height of the buildings, this effect is also reduced, as the airflow has less height to navigate and less pressure to compensate between the buildings. Additionally, tall buildings can create significant turbulence at their base due to the interaction between fast-moving winds at higher altitudes and the low-speed zones near the ground.
It is also understood that when buildings are placed too close together, air must pass through a confined space, increasing its speed to compensate for the reduced width. By increasing the spacing, the air can flow more freely, thus reducing its acceleration.
These phenomena do not occur in the baseline scenario, which is a positive outcome. However, in this case, the air becomes somewhat trapped between the buildings, with little circulation, which intensifies the urban heat island effect. Our aim is to slightly increase airflow between the buildings without creating turbulence or strong wind gusts. Therefore, we will avoid constructing taller and closer buildings.
Ideally, the airflow between the buildings should mimic the natural conditions found outside the Innovation Park. To achieve this, we have decided to slightly lower the height of the buildings and increase the spacing between them, aiming to recreate an environment that closely resembles a natural setting.

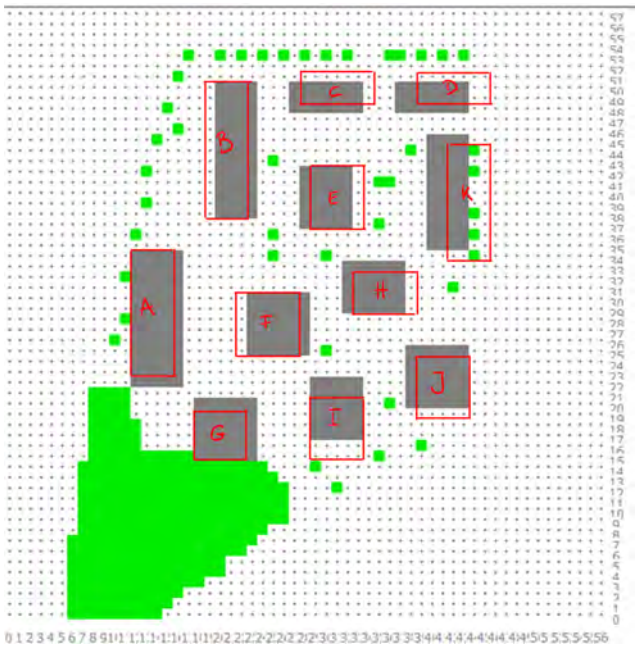

Figure 21: Modifications.

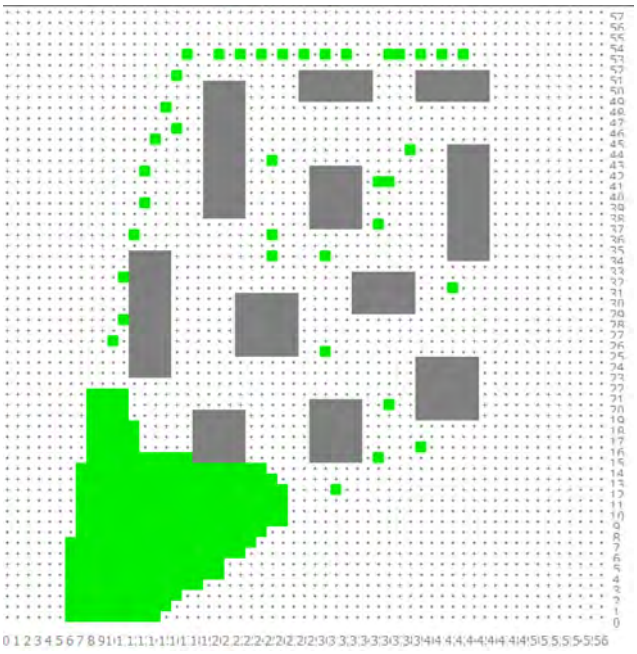

Figure 22: New design.

We have therefore reduced the height of each building by 2 meters. Buildings A and B are now 12 meters tall, building C is 14 meters, building D is 11 meters, and buildings E, F, G, H, I, and J are 20 meters tall. We also tried to space the buildings apart, slightly moving or resizing them as shown in the image above, with the red lines indicating the new building locations. The new urban morphology results in a significant loss of interior space in the buildings. To compensate for this lack of space, we will construct underground facilities to accommodate additional premises.

A drawback of lowering the height of the buildings and increasing the spacing between them is that there will be less shade between them, which could raise the temperature and thus reduce comfort. However, these building

modifications would likely not be implemented on their own. Trees would also be added, which would provide additional shade.

3.1.2 Results and comparisons with base case simulation

After implementing these morphology changes in ENVI-MET, we ran a new simulation. We will now analyse the results to determine which option offers the best thermal comfort.

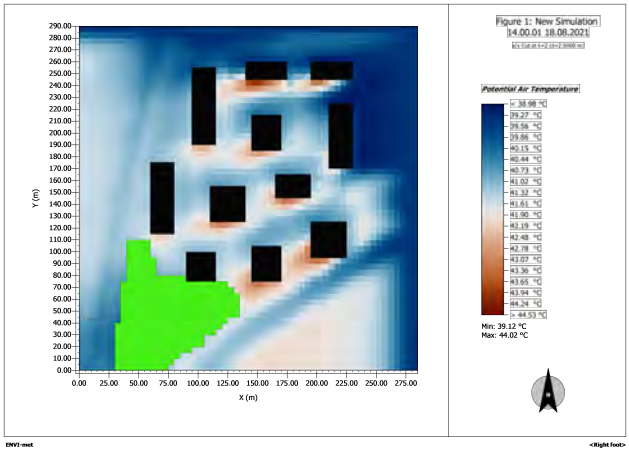

It will be easier to put the base case by the side or have a comparison graph showing the delta value.

Figure 23: Potential Air Temperature 2 PM.

We are looking at the potential air temperature, as in the base case, and we notice that it is lower with these modifications than in the base case. Indeed, there are many more areas where the temperature is below 40°C compared to the base case.

The maximum temperature is 44.02°C, whereas for the base case it is 43.75°C. So, it is slightly higher with my modifications than in the base case, but when we look at the heat distribution on the graph, we can see that it is only in very, very small areas. Therefore, this small increase is negligible.

The temperature has not drastically dropped, and several other changes would be needed for this to happen, but there is still a small decrease.

This could be due to the reduction in the urban heat island effect. Shorter buildings generally have a smaller surface area exposed to the sun and, as a result, generate less heat from the absorption of solar radiation. There is less heat accumulation, and therefore the potential air temperature decreases slightly.

The distribution of heat is also a bit more homogeneous with shorter and more spaced-out buildings, as there is less shading. We also notice that there are fewer large temperature changes compared to the base case. Furthermore, since the buildings are farther apart and there is more space, heat will dissipate more quickly during the night, for example.

It is also possible that this additional space creates better air circulation; ventilation can be improved, which increases the dispersion of heat. We will check this with the graphs on wind speed.

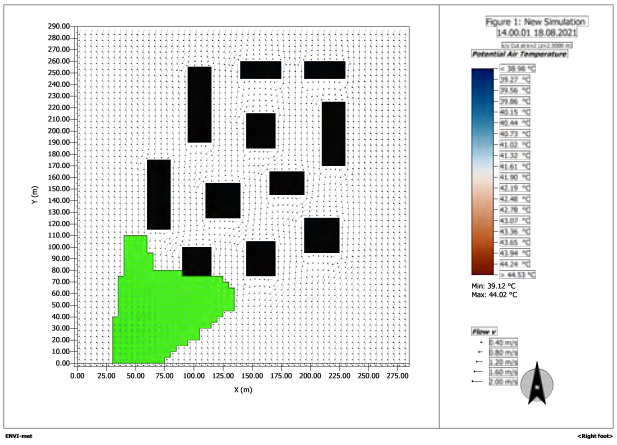

Figure 24: Wind Vector.

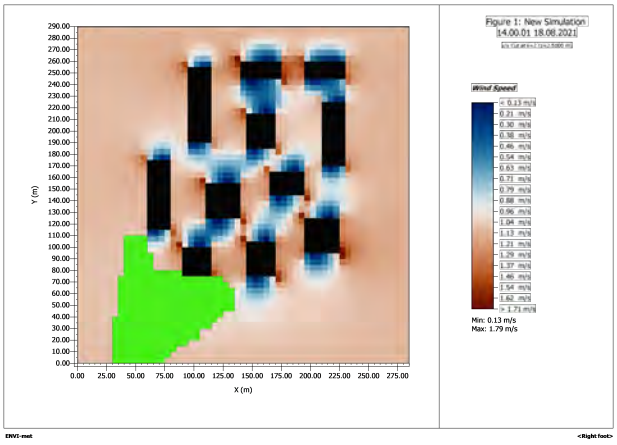

Figure 25: Wind Speed.

Indeed, we can see from the wind speed graph that there are fewer places where the air is completely still (i.e., where the wind speed is zero) compared to the base case. However, we also notice that the maximum wind speed is lower than in the base case. This shows us that the wind distribution is more uniform than in the base case, which is somewhat favorable. The changes are, once again, not huge, but there is still a difference.

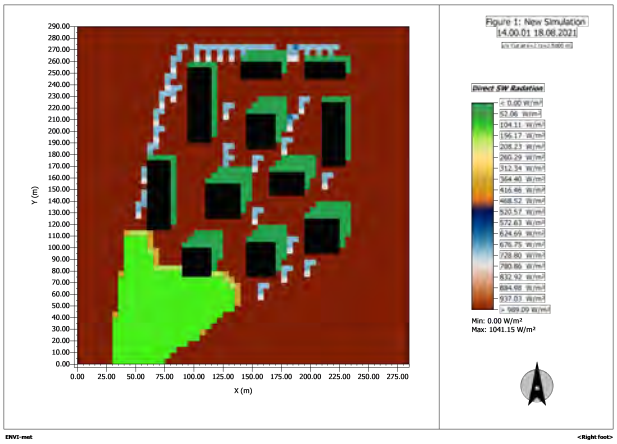

Figure 26: Direct SW Radiation.

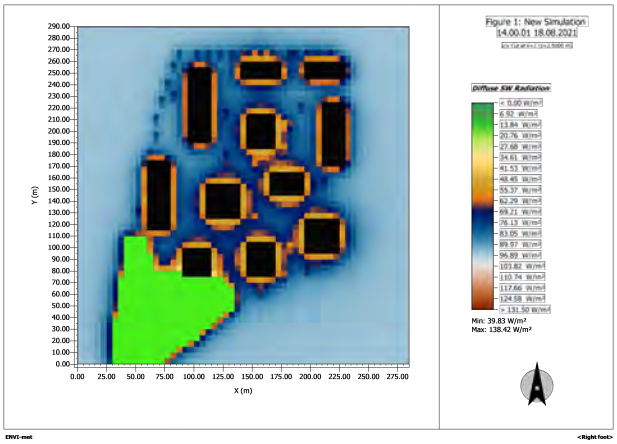

Figure 27: Diffuse SW Radiation.

For radiation, we notice that the direct radiation graph is exactly the same as the base case, which is not surprising because it represents light and energy coming directly from the sun, the portion that reaches a surface without dispersion.

For diffuse radiation, we observe from the distributions on the graphs that the values are slightly higher with our modifications, between the buildings, compared to the base case. If the diffuse radiation is higher, this implies a slight reduction in extreme temperatures, as we have already noted in the potential air temperatures, because more sunlight is dispersed, which can lead to a more homogeneous distribution of heat.

Link from higher diffused radiation to reduction in temperature not entirely right.

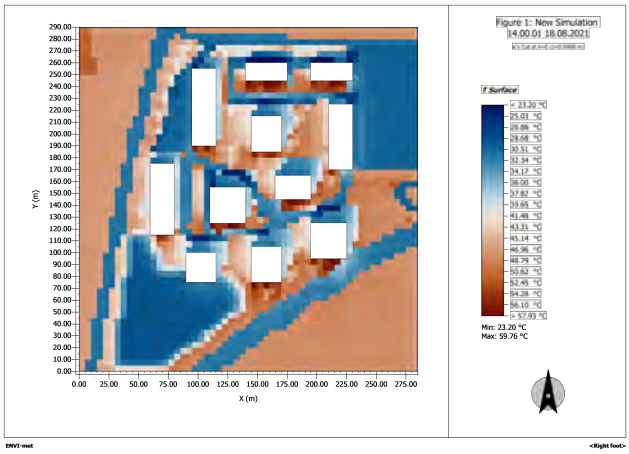

Figure 28: T Surfaces.

This better ventilation and diffusion of radiation also helps to slightly reduce the surface temperature, as we can see in the graph above. Indeed, in the base case, the ground temperatures ranged from 25.8 to 59.8 degrees, whereas here they range from 23.2 to 59.8 degrees. Additionally, there are more areas where these temperatures are a bit lower.

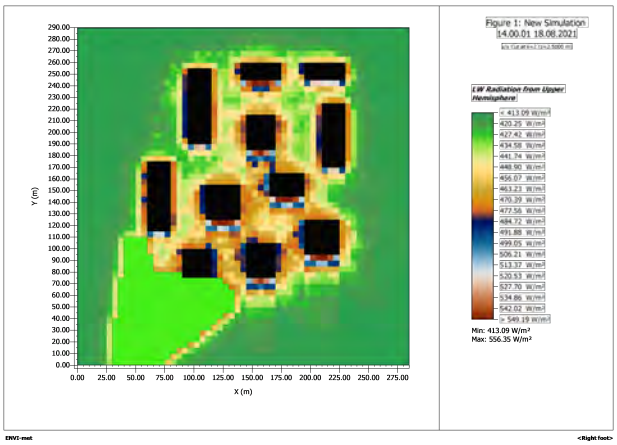

Figure 29: LW Radiation from Upper Hemispher.

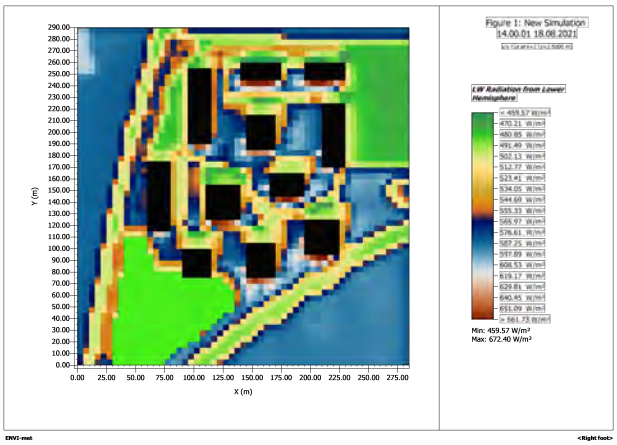

Figure 30: LW Radiation from Lower Hemispher.

It is noticeable that, with the changes I made to the Innovation Park, the LW Radiation Lower Hemisphere is slightly lower than before in certain areas, and the LW Radiation Upper Hemisphere is also somewhat weaker in a few areas compared to the baseline scenario.

The observed reductions in LW Radiation Lower Hemisphere and LW Radiation Upper Hemisphere may be due to a reduced ability of buildings to trap heat, better thermal dissipation through improved ventilation, and a more uniform distribution of heat within the environment. These changes contribute to a reduction in the urban heat island effect and an overall improvement in thermal comfort.

The modifications made to the city (reducing the building height and increasing the spacing) therefore seem to have a positive impact on heat management, with a decrease in thermal concentration and better air circulation, which leads to a reduction in ambient temperature and an improvement in thermal well-being in the area.

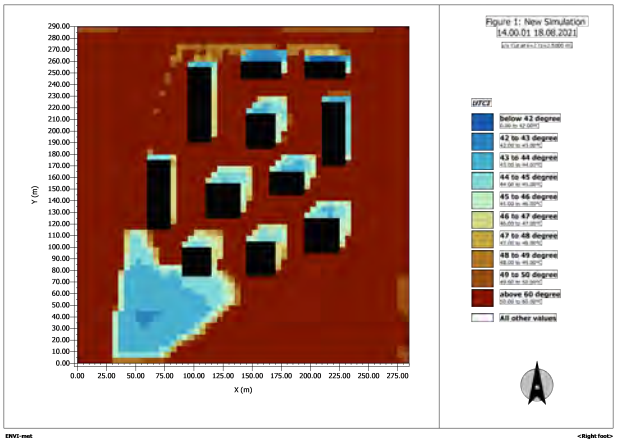

Figure 31: UTCI.

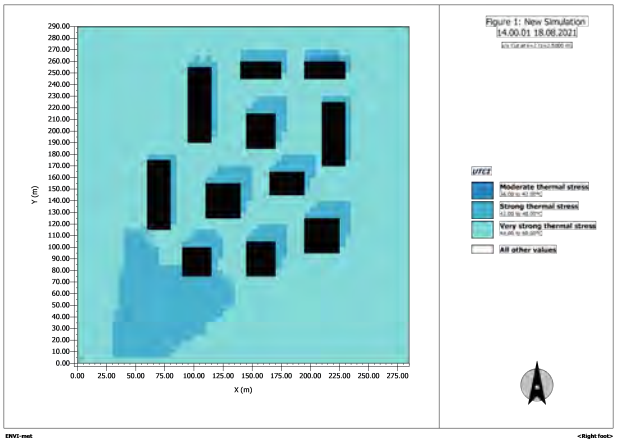

Figure 32: UTCI Thermal stress.

Here are the UTCI graphs. We can observe that they do not change much compared to those of the base case. This can be explained by the fact that the changes made to the innovation park, although they improve aspects like ventilation and thermal dissipation, are not sufficient to substantially modify the UTCI, as this index depends on several complex and interconnected parameters. The temperature and ventilation changes are not large enough to significantly affect the UTCI. Indeed, we also notice that the humidity does not change much with the modifications we made in this area, which could also explain the stability of this factor.

We can conclude that it is not really essential to make all these modifications to our space for such a small impact, especially since our changes would require more underground areas, resulting in a somewhat less pleasant environment inside the buildings.

3.2 Ground-environment interactions

This section of the report focuses on the interactions between the ground and its surrounding environment, emphasizing the thermodynamic and moisture exchanges that occur at the surface and subsurface levels. By analyzing various soil types and their distinct thermo-physical properties, we aim to understand how these factors influence surface and subsurface temperatures, ground heat flux, and evaporation rates.

Good analysis of material thermal properties.

3.2.1 Modifications for second simulation

Compared to the base site simulation presented earlier, we implemented four changes to the types of materials that make up the soil of the EPFL Innovation Park.

- The main roads surrounding the site we analyzed consist of a 4.5 m soil profile entirely made of asphalt. Examining this choice of material, it is evident that asphalt has a significantly higher thermal conductivity compared to natural soils, such as loam. This means asphalt absorbs and transfers heat more quickly, resulting in rapid heating and cooling cycles with pronounced daily and seasonal temperature fluctuations. Such a profile tends to heat intensely during the day, storing and releasing heat into the surrounding environment, thereby contributing to phenomena like the urban heat island effect. Additionally, asphalt is impermeable and does not retain water, leading to a complete absence of moisture within the profile. This eliminates the natural cooling effect of evaporation, further exacerbating overheating tendencies.
  Based on these considerations, for the new simulation, we propose a 4.5 m soil profile consisting of 30 cm of asphalt on the surface, underlain by sandy loam for the remaining depth. The expectation in this scenario is that while the 30 cm of asphalt on the surface will heat up quickly, the underlying loam will stabilize temperatures and mitigate the urban heat island effect. This is because loam acts as a thermal insulator, retains moisture, and allows for a more stable thermal gradient.
  In Figure 33, this material is represented by the colors red.

- The pedestrian pathways connecting buildings are initially made of concrete or sandy soil. Analyzing their thermo-physical properties reveals distinct differences between the two materials. Concrete generally exhibits good emissivity, allowing it to release accumulated heat, which contributes to nighttime urban warming. However, it has low permeability, hindering water infiltration and limiting evaporation, thereby reducing natural cooling. Additionally, concrete has higher thermal conductivity compared to natural soils and a moderate albedo coefficient, though darker concrete surfaces tend to absorb more heat. Sandy soil, on the other hand, has low emissivity, high permeability, low thermal conductivity, and a moderate albedo coefficient.
  Based on these considerations, in the second simulation, the sandy pathways will remain unchanged, while the concrete paths will be replaced with a surface of yellow brick stones. This material, used in a paved pathway, represents a thermally efficient alternative to concrete. It offers higher reflectance, elevated emissivity, and better permeability, helping to reduce overheating and enhance natural cooling.
  In Figure 33, the yellow brick stones is represented by the colors green, while the sandy is the colors yellow.

- The EPFL Innovation Park features a large parking lot made of concrete. Based on the thermal properties of this material discussed earlier, a combination of reflective, permeable, and vegetated paving is one of the best solutions for an urban parking area. This choice optimizes emissivity and reflectance, improving the overall urban thermodynamics. For this reason, we initially considered proposing a parking lot made of Turfstone (Figure 84), a paving system that combines permeable concrete blocks with spaces for grass. This solution would be practical for vehicle access in all weather conditions while providing vegetation coverage that reduces heat accumulation and promotes water infiltration. However, due to the complexity of modeling this type of pavement in ENVI-MET, we opted for a light concrete pavement instead. While it maintains good structural strength, this alternative offers advantages in terms of thermal insulation.
  In Figure 33, the light concrete is represented by the colors purple.

- Regarding the spaces around the buildings, which are initially made of concrete, we decided to replace them with basalt or granite, as these materials offer superior durability, thermal management, aesthetics, and potential permeability compared to concrete. For the simulation, we chose to apply granite in these areas, as it promotes water drainage—an important factor given the proximity to the buildings. Additionally, granite provides greater sustainability, offering increased resistance and durability while being easily recyclable. In terms of thermal capacity, it helps maintain a more stable surface temperature.
  In Figure 33, this material is represented by the colors orange.

Making four types of changes to the soil within a single simulation might seem excessive; however, in this case, the changes are highly localized. This approach allowed us, as we will see shortly, to achieve meaningful results while maintaining the ability to analyze each change independently and in comparison to the baseline scenario.

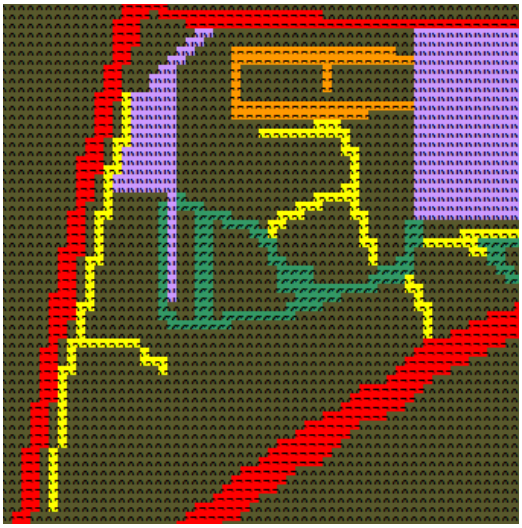

Figure 33: Soil profile for the ground-environment interactions simulation.

Legend: asphalt (red), yellow brick stones (green), sandy (yellow), light concrete (purple), granite (orange).

3.2.2 Results and comparisons with base case simulation

After implementing these material changes in ENVIMET, we ran a new simulation. We will now analyze the results to determine which option offers the best thermal behavior.

For air temperature, the results are presented in Figures 34 and 35 for both 2 PM and 4 PM. The temperature values range from 39.47°C to 44.16°C at 2 PM, and from 39.35°C to 47.99°C at 4 PM. While the minimum temperatures remain almost unchanged, the maximum temperatures are slightly higher than those in the base case simulation. For example, a closer examination of the asphalt areas reveals that in this second simulation, the red hues are more intense, particularly at 4 PM, indicating consistently high but slightly increased temperatures. Thus, for air temperature, this change did not yield positive results. In contrast, regarding the air temperature between the buildings, this new simulation shows more homogeneous temperature distribution in these areas. Additionally, the light concrete parking lot creates noticeably cooler air zones. To explore this further, we conducted a detailed analysis of air temperature variations in this area throughout the day. Graph 36 reveals that the highest recorded temperature (T = 47.99°C) did not occur in the parking lot. This outcome may be attributed to factors such as the material's reflectance (albedo). The curve also highlights that while concrete absorbs a significant amount of heat during the day, it releases this heat at night, resulting in a pronounced thermal gradient. This nighttime heat release contributes to warming the surrounding air during the evening and nighttime hours, further intensifying the urban heat island effect.

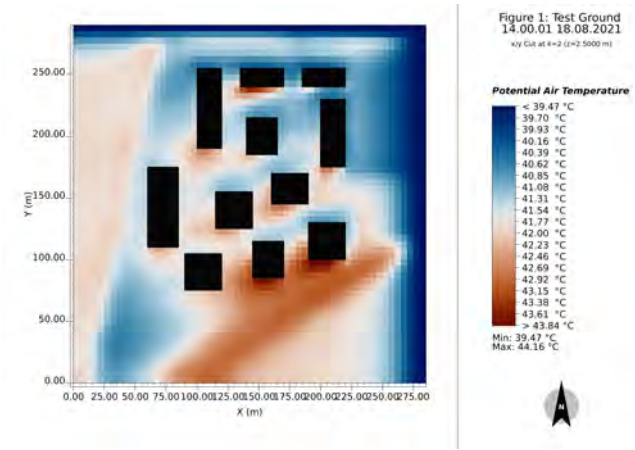

Figure 34: Potential Air Temperature 2 PM.

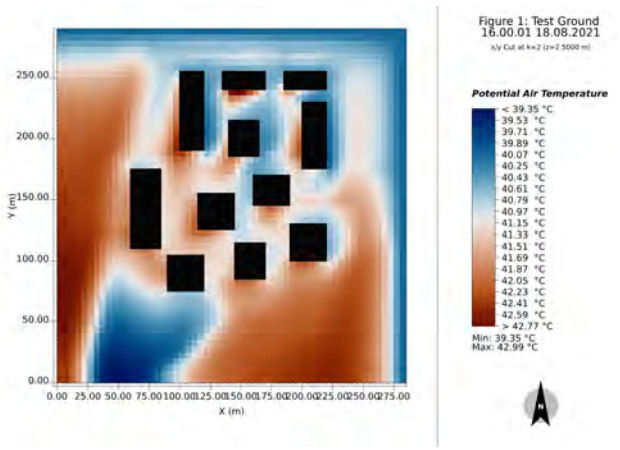

Figure 35: Potential Air Temperature 4 PM.

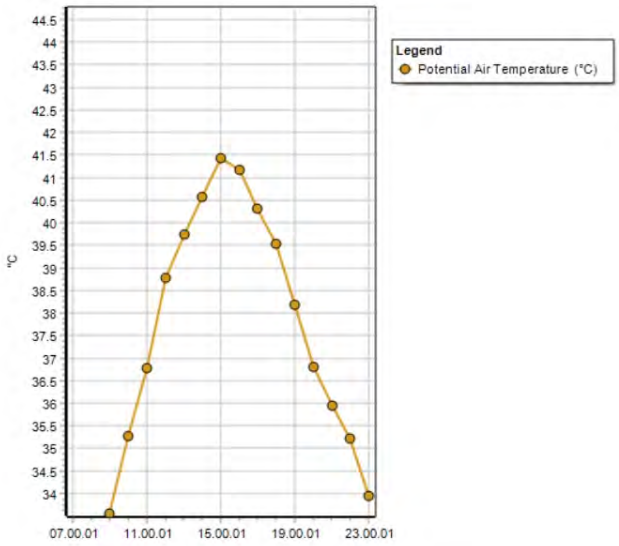

Figure 36: Air temperature variations in the parking area over the course of a day.

For the distribution of relative humidity, the results are presented in Figure 37, with values ranging from 39.81% to 48.51%. These values are almost identical to those in the base case simulation, as is the positioning of areas with lower and higher humidity. The highest relative humidity levels are still located in the bottom-left corner, where vegetation is present. The only significant difference is the noticeable decrease in humidity levels in the parking area. Interestingly, this reduction in humidity is accompanied by a decrease in air temperature in the same area. This suggests that the material changes made to the parking lot have improved its thermal performance.

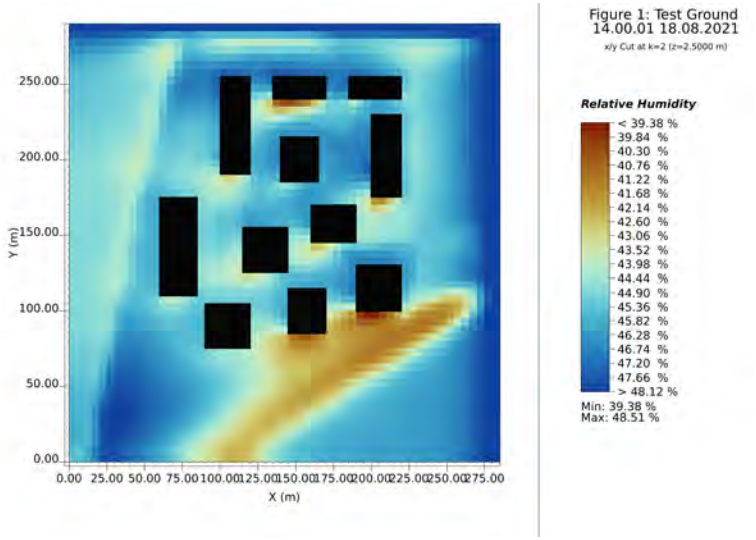

Figure 37: Relative Humidity.

For the surface temperature distribution, the results are presented in Figure 38, with values ranging from 23.08°C to 50.60°C. The maximum temperature has decreased by approximately 10°C compared to the initial simulation, resulting in lower temperatures in the asphalt areas. This indicates that using asphalt with a mixed stratification of sandy loam effectively stabilizes surface temperatures and mitigates the urban heat island effect. Additionally, we observe a lower average temperature in the areas between buildings. Interestingly, the ground near the north-facing façades of the buildings is significantly cooler compared to the other three façades, highlighting the influence of orientation on surface temperature.

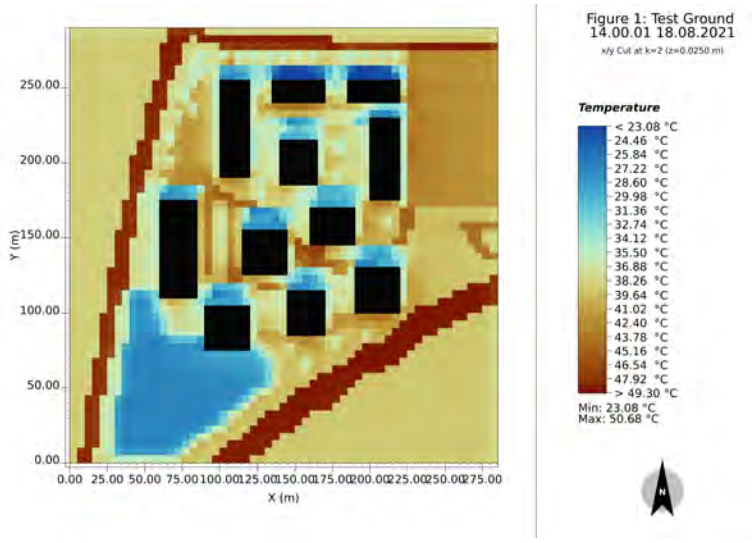

Figure 38: Surface Temperature.

In conclusion, this analysis of ground-environment interactions suggests that while the EPFL Innovation Park is already composed of relatively effective materials, certain modifications would be beneficial for the future. First and foremost, the parking lot would be significantly improved if made of light concrete, as it demonstrates superior thermal behavior. Regarding the pedestrian pathways between the buildings, they already perform well thermally, and using yellow brick stones or sandy soil would be an optimal choice. The final decision can depend on practical utility and specific requirements. On the other hand, granite near the building façades is relatively ineffective from a thermal perspective, as the temperature in those areas is largely influenced by solar orientation rather than material properties. Finally, for the asphalt roads, a new simulation should be conducted to strike a balance between the two scenarios already analyzed. This would help identify a compromise that optimally improves both surface and air temperatures in these zones.

Extensive analysis of the thermodynamic aspects of water body intervention, good connection between design principles and your practice implications and results.

3.3 Water body - environment interactions

This section examines the influence of water bodies on various parameters of the urban microclimate at the EPFL Innovation Park. The primary focus is to evaluate how incorporating water elements can enhance thermal comfort, reduce local temperatures, and create Urban Cooling Islands (UCI). In addition, the locations of the water bodies are determined from the basic site simulation according to different parameters. These locations will then be evaluated depending on their effectiveness as determined by the ENVI-met simulations.

Incorporating water bodies into the base case simulation is expected to leverage their lower surface temperatures compared to the surrounding urban area, enabling them to function as cooling sinks. Additionally, water evaporation is anticipated to elevate air humidity levels, which, depending on the regional context, may positively impact local thermal comfort. The wind patterns can influence these localized environmental changes. The thermal properties on EPFL Innovation Park site will be analyzed and validated through the simulation results, which will be discussed in detail.

To explore these dynamics, the analysis investigates interactions between water features and environmental parameters such as wind, solar radiation, air temperatures, and vegetation. The integration of water bodies aims to mitigate the Urban Heat Island (UHI) effect by combining water elements with vegetation and optimizing their arrangement relative to pre-existing urban structures.

3.3.1 Modifications for second simulation

In the second simulation, water bodies were introduced into the base site scenario. Shallow fountains were placed near office buildings and in the parking area. While fountains can disperse sprayed water or mist carried by the wind, these effects were not included in the simulation and will be discussed further. Additionally, the water features were designed and positioned to :

- Lower air and surface temperatures while increasing humidity levels to reach an improvement on the Universal Thermal Climate Index (UTCI).
- Interact synergistically with surrounding vegetation, urban form, and environmental factors such as wind direction, solar radiation and shading.

Guidelines for placement and design of water bodies

As we have just introduced, water features should be strategically placed near buildings to cool adjacent facades, thereby reducing heat storage in building materials and enhancing thermal comfort through evaporation. However, they should not be placed in shaded areas where insufficient solar radiation limits evaporation. Overall, water elements should maintain an optimal reflective and resonant distance from buildings.

A synergy between water and vegetation can significantly enhance cooling effects. Combining water bodies with trees or shrubs promotes cooling through evapotranspiration and increased humidity. Positioning water features close to trees amplifies shading effects while lowering transpiration-related leaf temperatures. We deal with the environmental interaction parameter in detail in Section 3.4.

Sunlight exposure is crucial for maximizing the cooling potential of water features. These elements should be located in sunlit areas to enhance evaporative cooling, with partial shading from trees to balance water loss.

Urban canyons and wind corridors also play a critical role. Aligning water features with prevailing wind directions facilitates the distribution of cooler and more humid air. Conversely, placement in narrow, poorly ventilated areas should be avoided, as such conditions could trap humidity and increase discomfort.

Finally, parking areas, identified as hot-spots in the baseline scenario, present an opportunity for thermal mitigation through water features. Incorporating such elements into parking zones requires a redesign of these spaces, as directly placing a fountain in the middle of a parking lot is not a practical solution. This intervention was tested to assess its feasibility in reducing thermal discomfort in these areas.

In this individual case of the water bodies simulation, we cannot modify some parameters such that the volume of vegetation or the morphology of the building. As a result, we design the best possible location for the water bodies according to the urban characteristics of the base site.

Design parameters for ENVI-Met simulation

The ENVI-met logiciel represents water bodies as a specific type of soil layer. We incorporated the following design parameters :

- 6 fountains with different shapes : 3 square fountains (10m x 10m), 2 rectangular fountains (15m x 5m) and a last one in angle with a surface of 75 m^2 to deal with the pre-existing vegetation.
- The location and the shape are selected to optimize the distribution and the diffusion of cooling. These parameters are illustrated in Figure 39.
- Simplified soil layers composed of :
  - 50 cm of water to simulate the depth of the fountain ensuring safety,
  - 50 cm of cement concrete as the structural base, ensuring waterproofing, and
  - Remaining layers up to 450 cm composed of the site's native sandy loam soil.

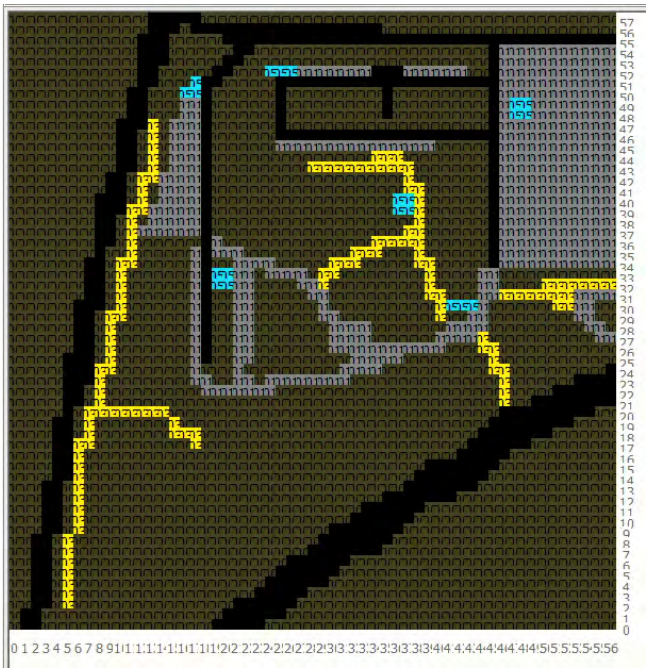

Figure 39: Location and shape of water bodies on the analysed site of the EPFL Inovation Park.

3.3.2 Result and comparisons with base case simulation

After implementing these design parameters in ENVI-Met, the results of the simulation were analyzed based on four key parameters: potential air temperature, relative humidity, surface temperature, and UTCI (Universal Thermal Climate Index). Each aspect was evaluated based on its relevance to the analysis, with and without the inclusion of fountains, comparing localized and overall effects across the simulation area at specific times or locations.

Potential Air Temperature and Relative Humidity

The addition of fountains significantly influenced the potential air temperature in their vicinity. As shown in Figures 40 and 41, cooling effects were localized around the fountains, with noticeable reductions of 1 to 3.34 °C depending on areas compared to the base case. The cooling effect was more pronounced near the parking fountain, which created a cold zone extending along the wind direction, as indicated by the wind patterns in the base simulation (Figures 11 and 13). Globally, a cooling effect is observed in open areas, with its diffusion generally following the wind direction and varying based on wind speed and intensity.

Unexpectedly, a cooling effect was observed near the cantonal road, likely resulting from wind-driven diffusion originating from nearby fountains, primarily the parking fountain and potentially the one at position (215,155). Similarly, the cooling effect along the western road could be attributed to the fountain located in the northwest. However, these explanations remain hypothetical, based solely on the surprising data outcomes.

The overall reduction in air temperature across the entire simulation site was relatively modest, averaging approximately 0.57 °C. This limited variation can be explained by the localized nature of the cooling effect generated by the fountains. The observed changes in potential air temperature are primarily attributed to the water's ability to reflect solar radiation and absorb heat, effectively functioning as a thermal sink.

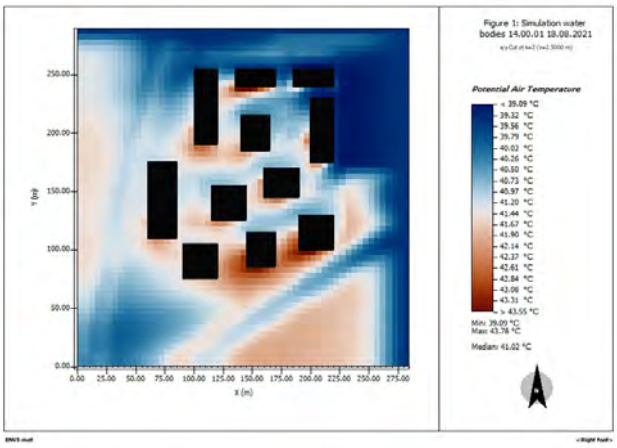

Figure 40: Result for the potential air temperature parameter for the simulation including water bodies.

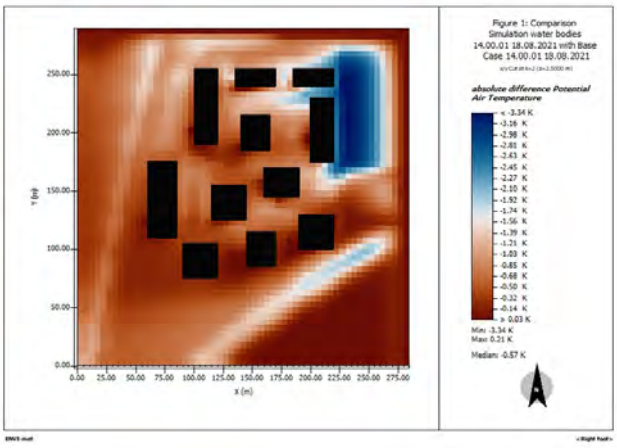

Figure 41: Comparison for the potential air temperature parameter between the simulation including water bodies (Observed data) and the simulation of the base case (Reference data).

Figures 42 and 43 illustrate the changes in relative humidity, which increased with the addition of fountains due to the evaporation process. On average, the overall humidity level rose by 2%, with a localized maximum increase of 8% near the parking fountain.

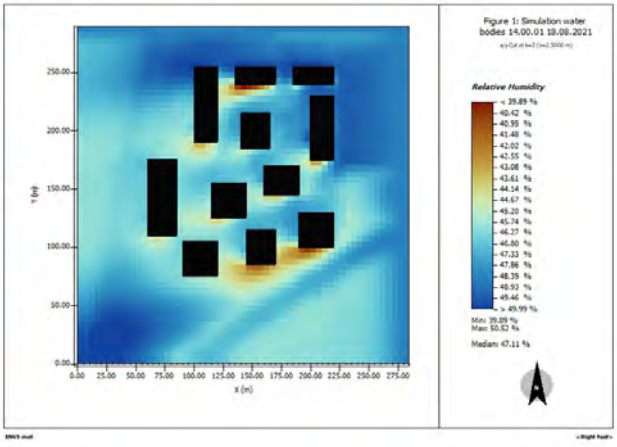

Figure 42: Result for the relative humidity parameter for the simulation including water bodies.

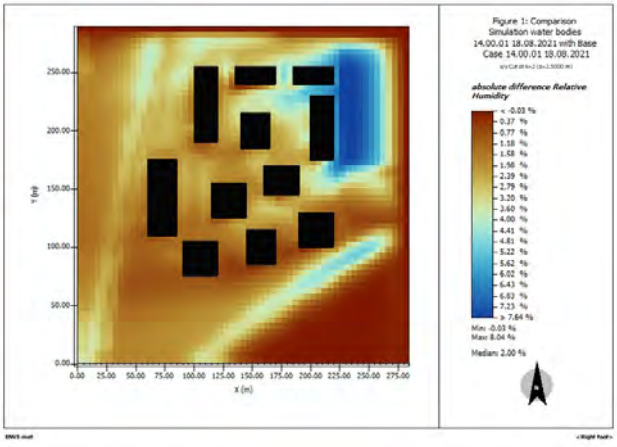

Figure 43: Comparison for relative humidity parameter between the simulation including water bodies (Observed data) and the simulation of the base case (Reference data).

Figures 44 and 45 present the temporal evolution of potential air temperature and relative humidity at a specific location on the map. These graphs demonstrate the influence of fountains on these thermodynamic parameters, showing lower air and surface[1] temperatures and higher relative humidity near the fountains. The results obtained for the simulation with water bodies were compared to the baseline reference map.

Interestingly, a shift in the timing of daily peaks was observed: the maximum air temperature shifted from 14:00 to 16:00, while the peak relative humidity was delayed until 18:00. This shift underscores the cooling and humidifying effects of fountains throughout the day, slowing the rise in air temperature and the corresponding decline in relative humidity.

[1]The impact on surface temperature will be discussed further; however, the conclusion is introduced here due to its correlation.

Fountains in narrower streets or surrounded by tall buildings showed limited influence due to restricted airflow and shading. In contrast, fountains in open areas, such as the parking lot and the northwest corner of the site, displayed more effective cooling, establishing a negative correlation between street width, building height, and cooling intensity.

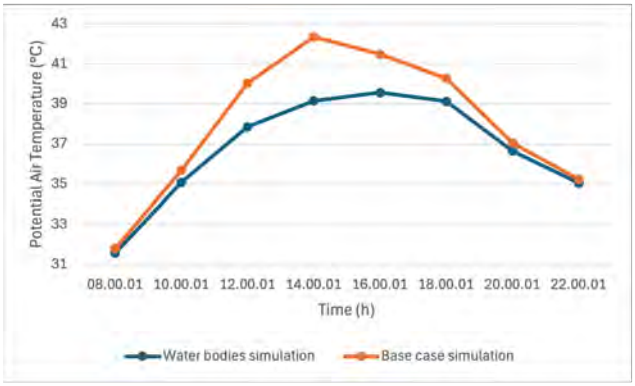

Figure 44: The potential air temperature (°C) along the day at the specific location of the parking area (on the fountain location in the simulation of water bodies). Comparison of the base case (orange) and the water bodies simulation (blue).

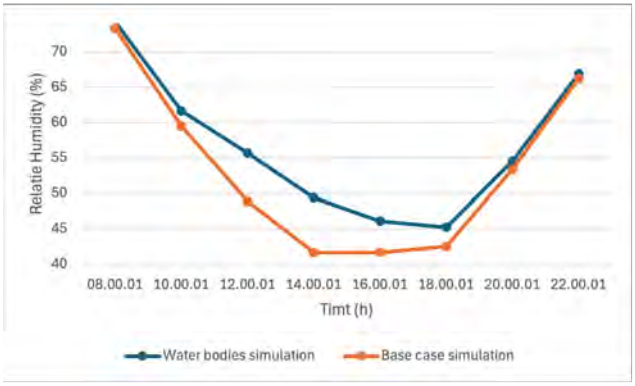

Figure 45: The relative humidity (%) along the day at the specific location of the parking area (on the fountain location in the simulation of water bodies). Comparison of the base case (orange) and the water bodies simulation (blue).

Surface Temperature

The presence of fountains also impacted surface temperatures, as illustrated in Figures 46 and 47. Fountains acted as cooling sinks, with nearby ground temperatures dropping significantly. For example, surface temperatures near the parking fountain decreased from 50 °C to 30 °C. However, the cooling effect was more noticeable in open spaces, such as the parking lot and the northwest fountain, whereas enclosed areas (e.g., near the northeast fountain at coordinates (185, 200)) exhibited limited impact due to restricted ventilation. This observation can be correlated with the wind vector and intensity map from the reference simulation (Figure 13).
Again, an unexpected finding was the cooling of asphalt roads, likely influenced by material properties and heat diffusion from adjacent areas. However, these explanations remain again hypothetical.

It seems that your intervention scenario may contain some modification of surface materials as reflected in the clear difference of T surface between two scenarios.

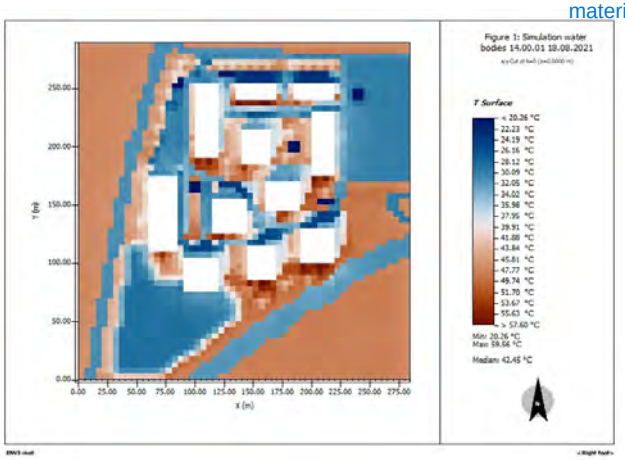

Figure 46: Result for the surface temperature parameter for the simulation including water bodies.

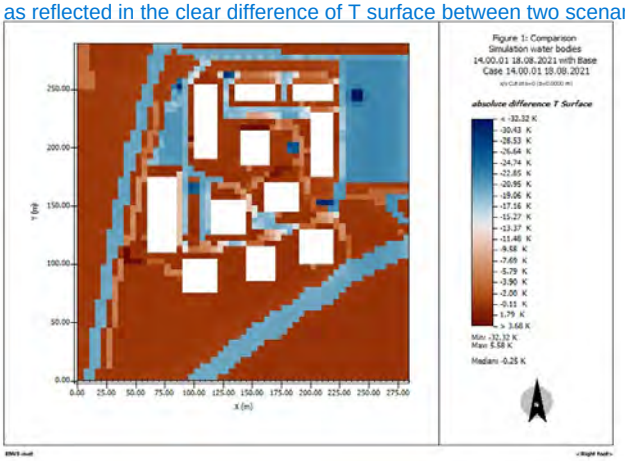

Figure 47: Comparison for surface temperature parameter between the simulation including water bodies (Observed data) and the simulation of the base case (Reference data).

Figure 48 provides a detailed comparison of surface temperature fluctuations over a day for different materials, including fountain water, parking concrete in the base case, and parking concrete in the modified scenario (water bodies simulation). While water temperatures remained nearly constant (increasing by only 1 °C), concrete temperatures showed greater fluctuations, with a 20 °C reduction at peak hours (14:00) in the presence of fountains. This effect was less pronounced in the morning and evening when ambient temperatures were cooler. As previously mentioned, a shift in the peak was observed. To gain a deeper understanding of water

surface temperature dynamics, only slight fluctuations were observed throughout the day. This stability can be attributed to the assumption that the water is continuously renewed, maintaining a consistent surface temperature. The slight increase of 1°C can be explained by the water's heat storage capacity and the reflection of solar radiation.

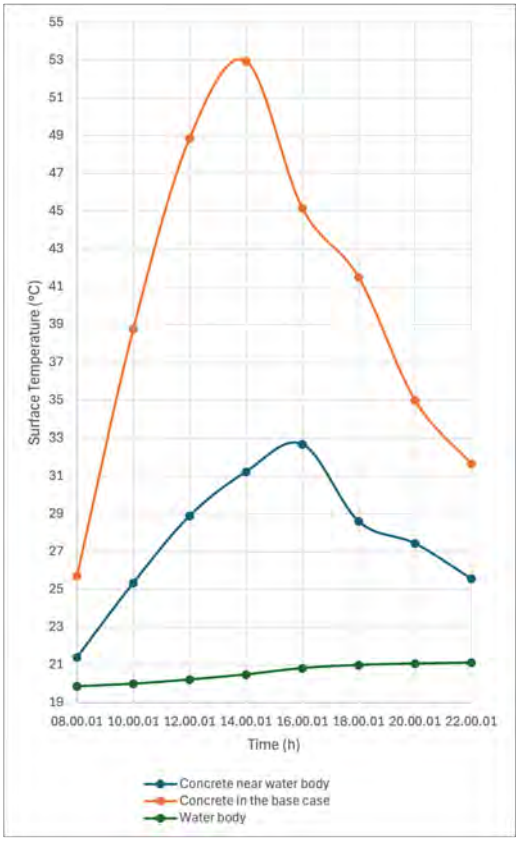

Figure 48: Comparison of the surface temperature on the parking along the day.

Urban Thermodynamic Confort Index (UTCI)

The impact of fountains on thermal comfort was assessed using UTCI (Figures 49 and 50). An influence was observed, with UTCI values decreasing by up to 3 °C in localized areas of the fountain. However, the overall site exhibited minimal change, with an average reduction of just 0.14 °C, indicating negligible overall impact. The cooling effects were primarily localized, improving thermal comfort only in the immediate vicinity of the fountains.

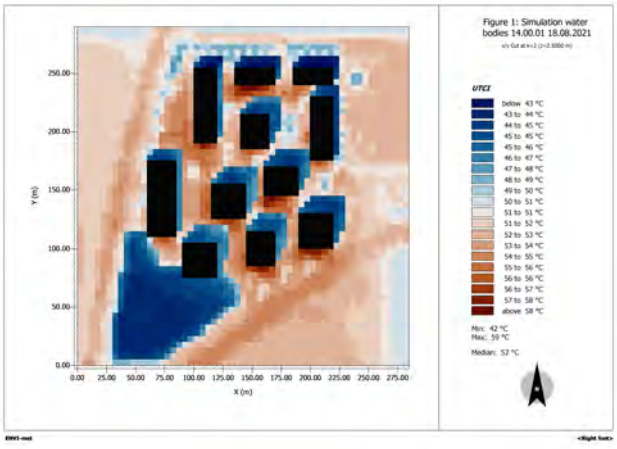

Figure 49: Result for the UTCI parameter for the simulation including water bodies.

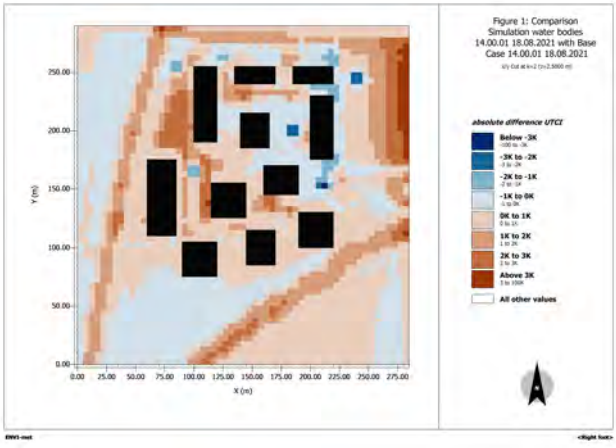

Figure 50: Comparison for the UTCI parameter between the simulation including water bodies (Observed data) and the simulation of the base case (Reference data).

According to a study[2], fountains with water spray can reduce temperatures by 1 – 2 °C, with effects extending tens of meters downwind. In this simulation, the cooling effects were similarly localized to areas within tens of meters of the fountains. Larger water features could potentially amplify the reduction in UTCI and other thermodynamic variables, offering more significant enhancements to thermal comfort.

Final conclusion of results

The simulation results emphasize the localized cooling and humidifying effects of fountains, particularly in open areas. Fountains reduce air and surface temperatures, delay peak temperatures, and increase relative humidity, improving thermal comfort in their immediate surroundings. Strategic placement and design of water features can maximize their cooling potential, reducing urban heat and enhancing comfort, especially in well-ventilated areas. However, the overall site impact remains modest, with average reductions being minimal. To enhance their effectiveness, optimizing fountain size, placement, and design is crucial. Larger water features or additions like water sprays could provide broader and more substantial thermal benefits. Excessive humidity in poorly ventilated areas also requires careful consideration to align designs with wind corridors.

This analysis underscores the role of water bodies as effective tools for urban microclimate mitigation when integrated with vegetation and thoughtful urban planning. Future studies could explore configurations such as varying water depths, shapes, or dynamic features like streams to identify the most effective solutions for improving urban thermal comfort.

[2]ETH Zürich study of *Strategies for cooling Singapore* [1]

3.4 Vegetation - environment interactions

3.4.1 Modifications for second simulation

Urban vegetation planning is an essential strategy to address the challenges of climate change, particularly in urban environments where occupants experience the combined effects of heat and solar radiation. This study, based on simulations conducted for a day on August 18, 2100, in the EPFL Innovation Park area, compares the effects of current vegetation with a projected vegetation composition for 2100. These analyses demonstrate how the addition and optimization of vegetation can transform local conditions, benefiting both the environment and the well-being of inhabitants.

Figure 51 illustrates the placement of different vegetation types used in our simulation.
Field maples (A9) are aligned along the main paths and in parking lots to provide shade and regulate temperature in summer while allowing light to pass through in winter. They also capture pollutants and support nesting birds.
Hazelnut trees (90), positioned near main roads and around buildings, create a natural barrier against noise and nuisances while promoting biodiversity by attracting squirrels and birds with their nuts.
Hedges (H2) delineate spaces between parking lots and parks, improving aesthetics and protecting nearby buildings from significant traffic noise. Hedges also serve as a valuable solution for biodiversity, providing habitats for local wildlife.
Grass (X) is installed in parks between buildings to offer comfortable and visually appealing recreational spaces.

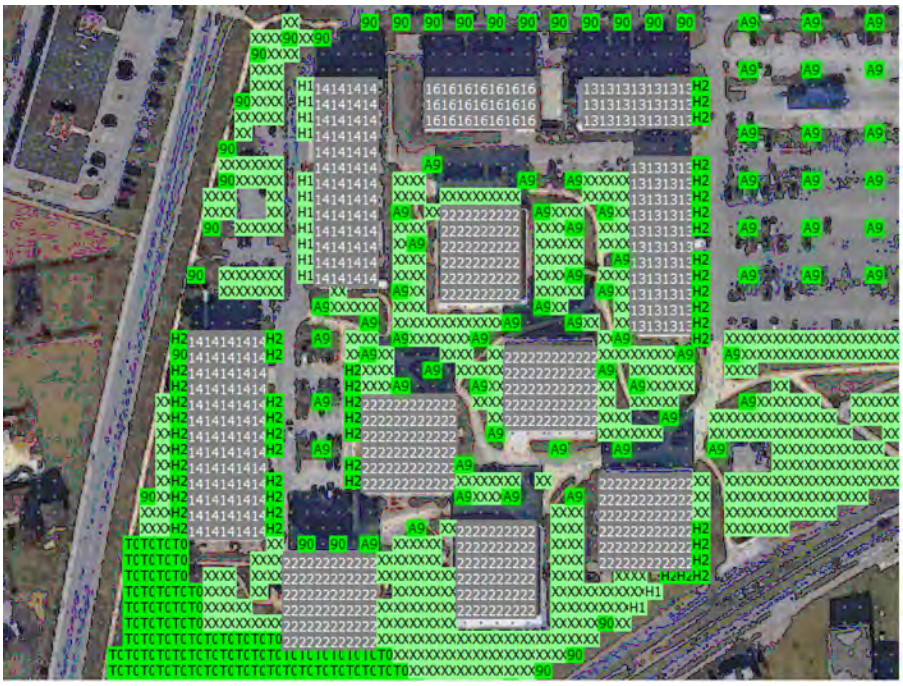

Figure 51: Placement of different vegetation types.

3.4.2 Results and comparisons with base case simulation

Air temperature analysis:
We first analyze the effect on air temperature. The results show a significant reduction in air temperature in areas where the vegetation projected for 2100 is implemented, like for example right next to the building in the middle. We see that throughout the day the temperature is reduced (figure 52). The difference is greater during times of day when the temperature is high. These decreases, up to 5°C, are particularly pronounced in spaces between buildings, such as parks and pedestrian zones, where the presence of a denser canopy acts as a natural barrier against the urban heat island effect (see figure 53 and 54). This reduction is particularly beneficial in these areas as they are key locations for improving thermal comfort away from roads, in spaces where pedestrians walk. This decrease can be explained by two main mechanisms:

- **Natural shading:** Trees like the field maple and hazelnut, with their dense foliage, block a significant portion of direct solar radiation, reducing heat accumulation on urban surfaces.

- **Evapotranspiration:** This biological process, by which plants release water into the air as vapor, absorbs part of the ambient thermal energy, creating a cooling effect.

These combined effects make public spaces more pleasant for users, encouraging the use of pedestrian zones and parks even during hot days. Additionally, by planting trees in the upper-right parking lot, we observe a decrease in air temperature, a positive effect for cars that will heat less under the trees' shade. This contributes to improving not only the thermal comfort of individuals but also their overall well-being by reducing heat stress.

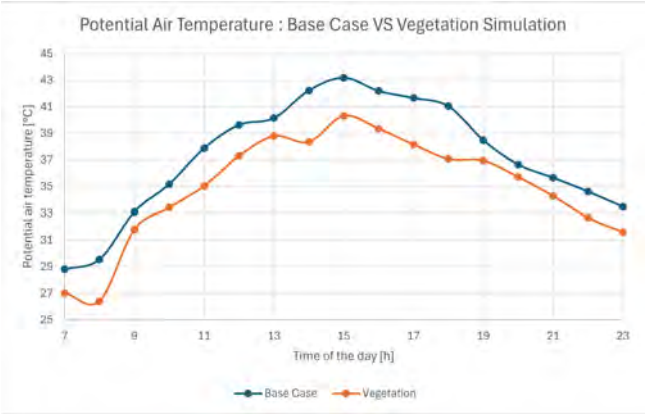

Figure 52: Potential air temperature vegetation vs base case.

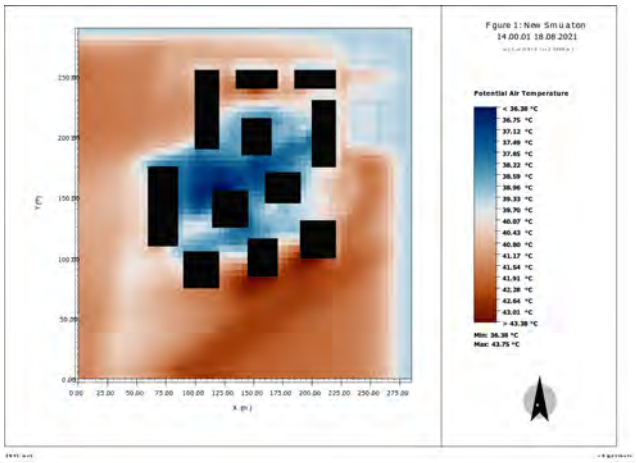

Figure 53: Potential air temperature at 2 PM.

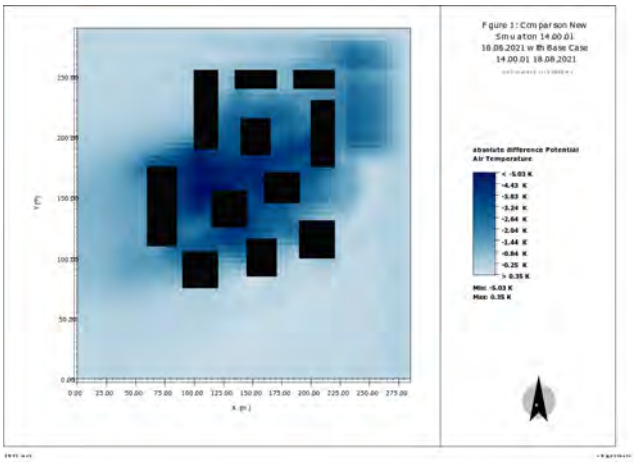

Figure 54: Potential air temperature air comparison.

Increase in Relative Humidity:

Another notable impact is the general increase in relative humidity in vegetated areas, reaching up to 60% in certain strategic locations, such as the spaces between buildings (Figure 55). Additionally, it is observed that relative humidity can be increased by up to 15% through the strategic placement of vegetation (Figure 56). This rise in humidity is beneficial for several reasons. First, it mitigates the effects of dry heat, typical of summer periods in urban environments, making the air more comfortable to breathe.

Moreover, this additional humidity promotes a natural thermal balance in the studied area. The evapotranspiration of trees, combined with improved rainwater management by hedges and shrubs, helps maintain coolness even during prolonged droughts. This is particularly relevant in a context where precipitation patterns may become more irregular by 2100. These results highlight the importance of selecting plant species capable of actively contributing to water and humidity regulation in more demanding future climates.

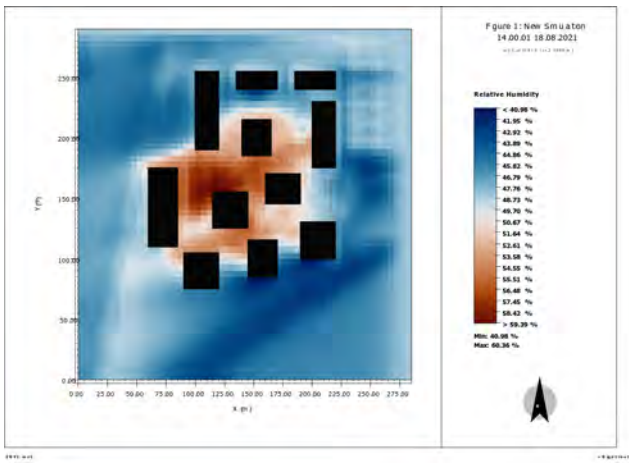

Figure 55: Relative humidity at 2 PM.

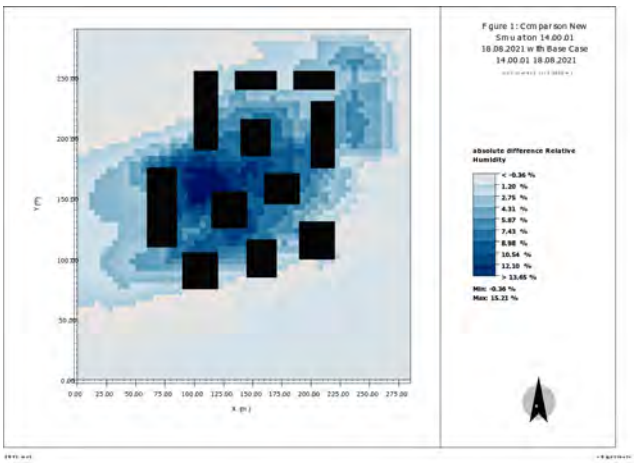

Figure 56: Relative humidity comparison.

Impact of Vegetation on Solar Radiation Distribution:

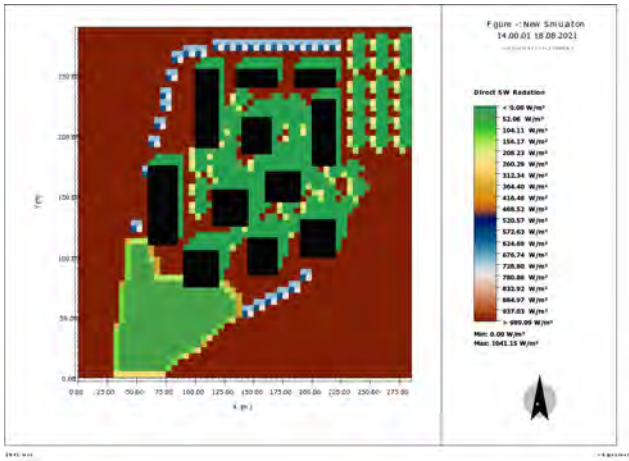

Figure 57: Vegetation - SW Direct Radiation at 2 PM.

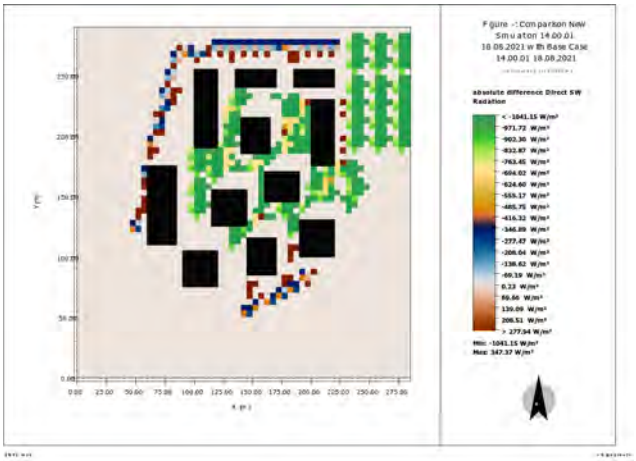

Figure 58: SW Direct Radiation Comparison.

Figure 57 and the comparative Figure 58 show the distribution of direct solar radiation after the addition of vegetation. A significant reduction in solar radiation exposure is observed in many areas due to the shading created by the vegetation.

Trees such as the field maple and hazel reduce exposure in key areas such as pathways, parking lots, and spaces between buildings. These areas, previously highly exposed, now benefit from better protection against direct solar radiation, limiting the warming of urban surfaces.

Additionally, the analysis of shortwave diffuse radiation (**SW Diffuse Radiation**) reveals notable changes. The hazel trees, with their lighter and more spaced-out foliage, act as better diffusers of solar light, thereby increasing the amount of diffuse radiation in their immediate surroundings. This contrasts with other types of trees, whose denser canopies block more light and reduce diffusion. This difference is particularly pronounced in the areas beneath these trees, where the shading is more significant, limiting the amount of light that can be diffused to the ground (Figure 59).

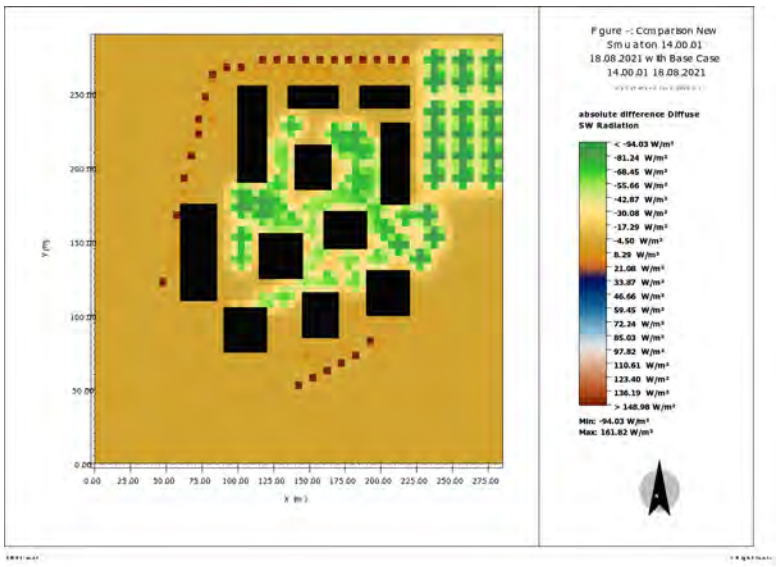

Figure 59: SW Diffuse Radiation Comparison.

For infrared thermal radiation (**LW Radiation**), contrasting results are observed between the upper and lower hemispheres:

- **LW Radiation Upper Hemisphere** (Figure 60)**:** A slight increase is observed. This is explained by the re-emission of radiation by the vegetation, which absorbs some of the thermal energy before sending it back to the atmosphere. Additionally, the dispersion of radiation by the leaves helps redistribute energy towards the sky.
- **LW Radiation Lower Hemisphere** (Figure 61)**:** A marked decrease is observed. This reduction is mainly due to the cooling of urban surfaces through shading and evapotranspiration. Cooler surfaces emit less thermal radiation, while the vegetation acts as a physical barrier, blocking some of the thermal radiation generated at the ground.

These combined mechanisms illustrate how vegetation redistributes radiative energy. By increasing thermal exchanges with the atmosphere, reducing heat accumulation at the surface, and dispersing solar radiation, it contributes to lowering local temperatures, improving thermal comfort, and mitigating the urban heat island effect.

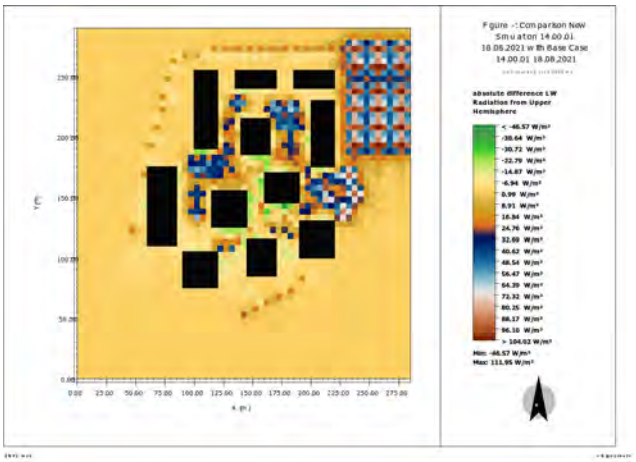

Figure 60: LW Radiation Upper Hemisphere Comparison.

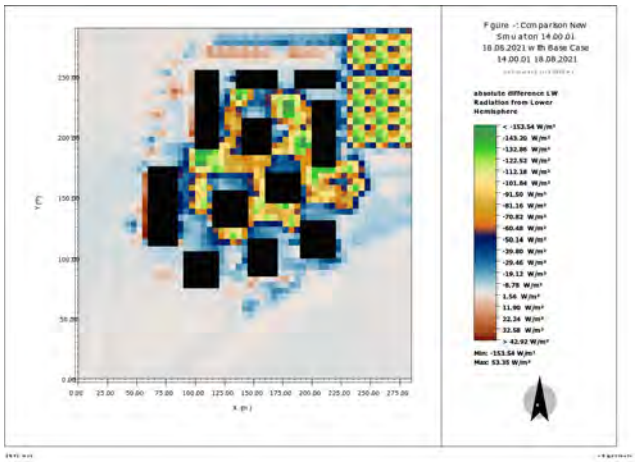

Figure 61: LW Radiation Lower Hemisphere Comparison.

Impact of Vegetation Addition on Thermal Comfort (UTCI):

Figure 62 shows the ranges of UTCI temperatures after the addition of vegetation, with variations ranging from "less than 39 °C" to "more than 50 °C." The analysis reveals a significant reduction in UTCI temperatures in shaded areas created by the new vegetation, compared to exposed zones. Spaces under the trees exhibit lower temperatures, highlighting the cooling effect of vegetative shading.

Figure 63 categorizes UTCI ranges into thermal stress levels, revealing notable improvements. Zones experiencing moderate thermal stress (36 °C to 42 °C) have expanded due to the increased vegetation, particularly around pathways, parking areas, and between buildings. These spaces benefit from reduced direct solar radiation due to tree shading, thereby improving thermal comfort.

In contrast, zones of strong thermal stress (42 °C to 48 °C) are primarily confined to remaining open areas, such as those without tree coverage. Thanks to the shading provided by field maples and hazelnut trees, these areas have seen a marked decrease in temperatures.

The addition of vegetation also influences areas exposed to very strong thermal stress (48 °C to 56 °C). These zones, previously dominated by impervious surfaces and heavily exposed to solar radiation, have experienced a significant reduction in thermal stress. Trees planted near buildings cast substantial shadows, and evapotranspiration further cools these spaces.

Moreover, the increase in the vegetative canopy plays a key role in dispersing solar light and reducing heat accumulation. Hazelnut trees, for instance, are strategically spaced to create light but diffuse shading, improving thermal comfort while maintaining pleasant brightness in certain areas.

These findings highlight the positive impact of greening strategies on urban thermal comfort. From an urban planning perspective, areas with high thermal stress benefit from the addition of green infrastructure, such as trees and hedges, which enhance shading and reduce ground-level temperatures. These solutions underscore the importance of thoughtful design to mitigate urban heat island effects and improve the well-being of city inhabitants.

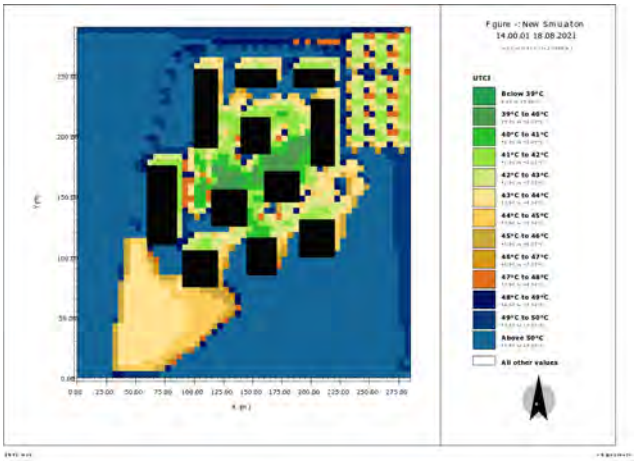

Figure 62: Vegetation - UTCI.

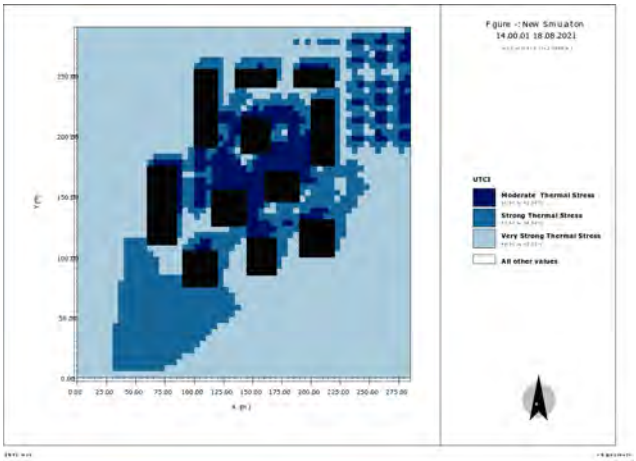

Figure 63: Vegetation - Thermal Stress (UTCI).

4 Integrated Microclimate Solution

4.1 Final Solution Proposition

Vegetation, soil and ground types, buildings disposal, and the role of water bodies in shaping the microclimate have been analyzed. Each element has been studied for its individual and combined impact on thermal comfort. With this understanding, the focus rests on developing the final solution by integrating these components into a cohesive design, aiming to reduce among others air temperature, radiation and above all thermal comfort. Figures below 64, 65, 66 respectively represent a 3D map of the integrated solution, a 2D visualization of soils and ground and the last one of buildings and vegetation.

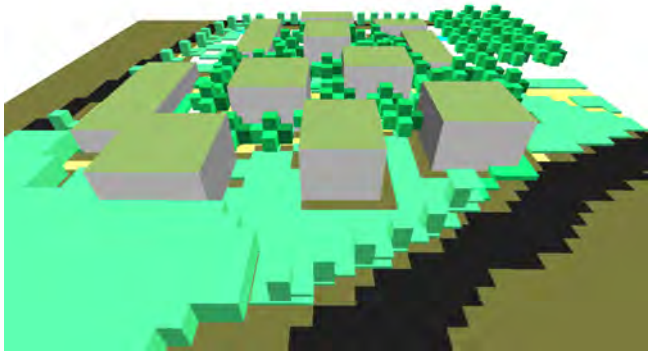

Figure 64: Integrated Solution - 3D Map.

Figure 65: Final Solution - Buildings & Vegetation.

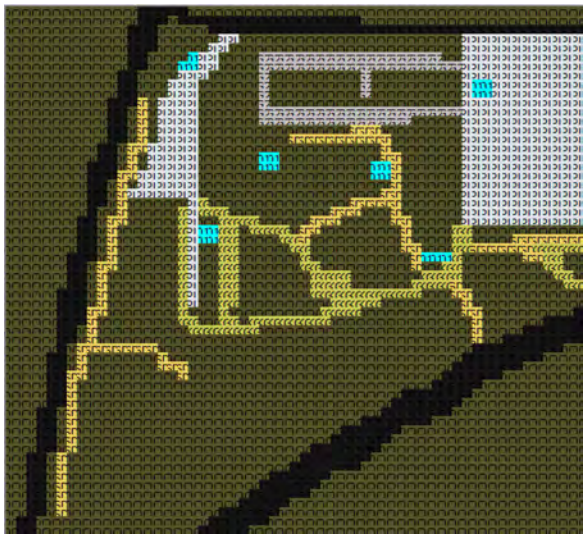

Figure 66: Final Solution - Soils & Ground.

Figures 65 and 66 above show that the disposition of the elements analyzed in the previous section hasn't changed much except for buildings and for some fountains. Heights of buildings has been reduced but the spacing between them has not, as it is not very feasible. Water Bodies have been placed near the vegetation. Indeed, the humidity generated by a fountain may help plants, trees and grass to stay in better shape, especially during very hot summers. Together, they work to reduce the Urban Heat Island (UHI) effect by increasing humidity and lowering air temperature. The fountain on the concrete pavement light (on the parking area) has remained here, as it contributes to cooling the parking zone next to the entrance of the Innovation Park. In fact, even if the concrete pavement light heats up less than the cement concrete, and that's already an improvement in itself, it still remains hotter than the purpose. Adding a fountain next to it acts as a cooling center. Together, they effectively reduce the Heat Island effect.

Even though this element hasn't been changed from the initial case, it is important to note their contribution for each other and for the microclimate. Plants need well-drained soil, which is the case of sandy soil, to avoid water stagnating around the roots, to prevent damaging vegetation's health. Together, the sandy soil and vegetation

create an efficient water management cycle, where the moisture transpired by plants is quickly dissipated by the soil, avoiding overheated or waterlogged areas. They collectively contribute to reducing the environment's capacity to store heat, which is crucial for limiting the effects of heat islands.

In Figure 64, there's a small difference visible that could also make a significant microclimate change. In fact, a green substrate combined with sandy loam has been implemented on the rooftops of the buildings. This element and not another one was added for the reasons that it offers great water retention capacity and sufficient nutrients for extensive or intensive vegetation. In terms of microclimate, it acts as natural insulation, reducing heat transfer between the building and the environment. It reduces the Urban Heat Island (UHI) effect through shade and evapotranspiration and decreases solar radiation absorption: plants absorb and reflect a portion of solar radiation, preventing it from directly heating the rooftop surface.

4.2 Simulation's Results and Comparison with Previous Scenarios

As the integrated solution is defined based on the previous scenarios, it is possible to simulate the model using the microclimate simulator "Leonardo". Note that the comparisons with EXCEL graphics in the following sections have been focused on a single grid pixel to avoid an excessive number of simulations. The selected pixel is located in the center of the innovation park, representing the area where our microclimate modifications are expected to be most effective and where pedestrian traffic is likely to be highest. For the following simulations, they all have been done at 2 PM (14h00) like the simulations in the previous sections.

4.2.1 Air Temperature

Nice comparison of different scenarios throughout the day. It would be good to visually show the selected sample point for this analysis.

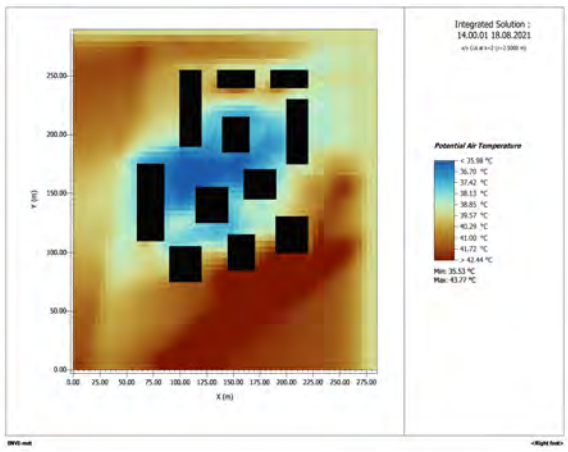

Figure 67: Integrated Solution - Potential Air Temperature.

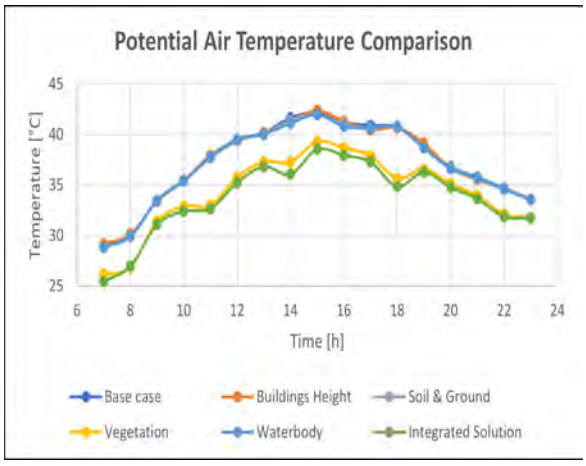

Figure 68: Integrated Solution - Potential Air Temperature Comparison.

As illustrated in Figures 67 and 68, there is a substantial temperature reduction. The minimum potential air temperature has dropped to 35.53 °C, compared to 39.47 °C in the base case, yielding a nearly 4 °C improvement. It is a significant and non-negotiable gain. However, this difference represents the maximum reduction observed. Across the park, there is a noticeable overall temperature decrease due to the strategically placed vegetation, which provides natural shading and promotes evapotranspiration. These mechanisms respectively reduce heat accumulation on urban surfaces and absorb part of the ambient thermal energy, creating a cooling effect.

It is worth noting that, in the initial scenario, the hottest area was located in the top-right corner, dominated by a large asphalt-covered parking lot. In this simulation, the addition of trees over this surface and a fountain nearon entrance of the park has resulted in significant improvement.

In comparison with previous scenarios, as shown in Figure 68, the selected pixel in the grid, not being located near a fountain or on a different soil type, exhibits a temperature similar to the base case. However, since the final scenario is influenced by the vegetation's cooling effect, the selected pixel shows a lower temperature overall. This demonstrates that, even without direct adjacency to vegetation, its cooling influence extends throughout the surrounding area.

4.2.2 Relative Humidity

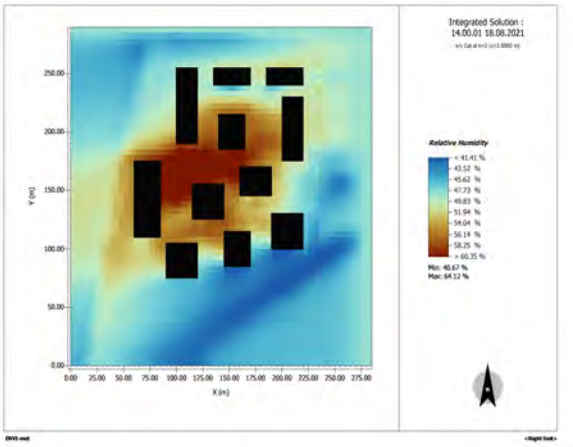

Figure 69: Integrated Solution - Relative Humidity.

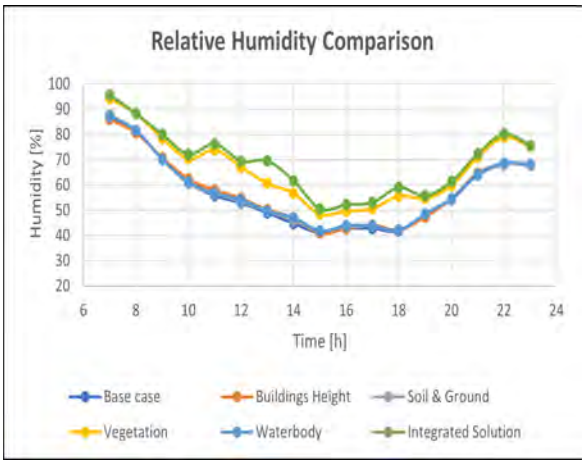

Figure 70: Integrated Solution - Relative Humidity Comparison.

As shown in Figure 69, this simulation illustrates the distribution of relative humidity across the final solution, with values ranging from 40.67% to a maximum of 64.12%. There is a noticeable increase in humidity within the park due to the implemented modifications. Specifically, the presence of water features, such as fountains, and vegetation contributes to significant moisture retention within the area.

An important observation from this simulation is that the relative humidity inside the park is higher than in the bottom-left corner, where a dense mass of vegetation is present. This is largely attributed to the additional presence of water in the park. In contrast, the humidity in the bottom-left corner is solely generated by vegetation, whereas the park benefits from the combined effects of vegetation and fountains distributed throughout the site.

In comparison to previous scenarios, as shown in Figure 70, the integrated solution achieves the highest relative humidity levels throughout the day, closely resembling those of the vegetation microclimate model. Similar to the potential air temperature results, the influence of fountains extends beyond their immediate neighborhood. Although the selected pixel is not located near a fountain, the final solution still exhibits higher relative humidity compared to the vegetation model. Furthermore, the integration of green substrates combined with sandy loam in the final solution likely contributes to this increase in relative humidity.

4.2.3 Surface Temperature

The simulation in Figure 71 shows the surface temperature distribution across the site, with values ranging from 19.96 °C to 58.96 °C. The coolest areas are observed near fountains and vegetation, particularly in the bottom-right corner, throughout the innovation park (mainly adjacent to buildings), and in the parking area. Conversely, the hottest regions are found on the roads, where asphalt's present, as it is a material known for its high heat retention and radiation properties.

The lower surface temperatures can be partly attributed to humidity, as the sandy soil absorbs moisture from tree evapotranspiration. However, they are primarily due to shading and the cooling effect of water surfaces. As shown in Figure 71, the coolest temperatures are observed beneath trees (notably in the parking area under each tree), around water fountains, and on the northern sides of buildings. This cooling on the north-facing surfaces is due to the buildings' height, which blocks direct sunlight from the south. By shielding these areas from solar radiation, the north-facing surfaces and their surroundings remain cooler.

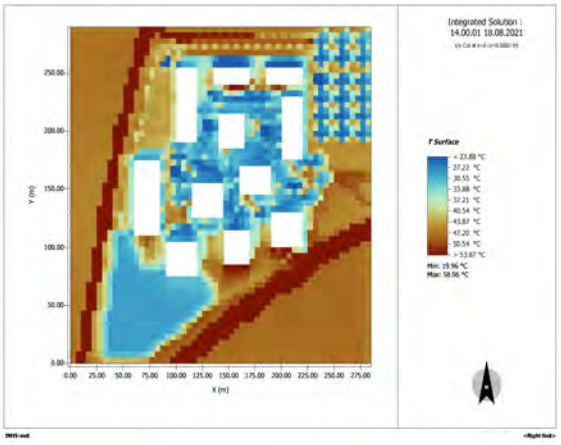

Figure 71: Integrated Solution - Surface Temperature.

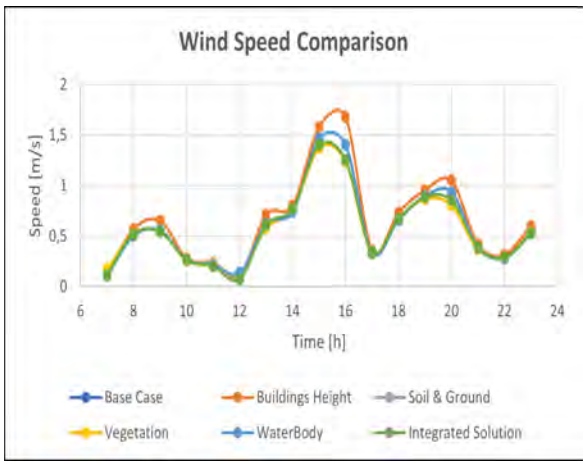

Figure 72: Integrated Solution - Wind Speed Comparison.

4.2.4 Wind

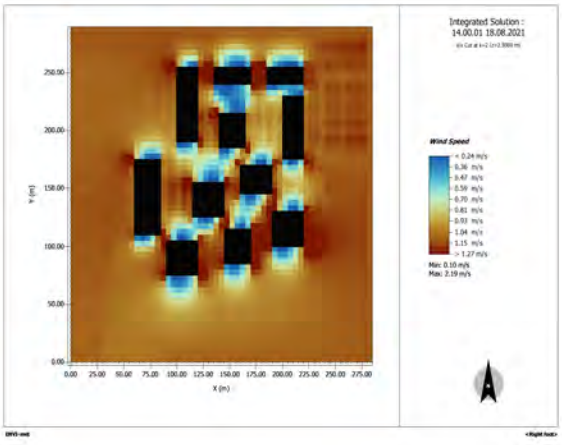

Figure 73: Integrated Solution - Wind Speed.

Wind direction should be visualised with arrows for easy understanding.

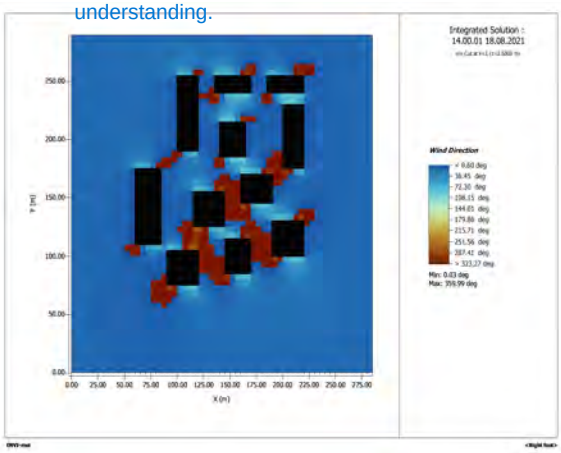

Figure 74: Integrated Solution - Wind Direction.

The simulation illustrates wind flow patterns across the site, with wind speeds ranging from 0.10 m/s to 2.19 m/s. These variations are primarily influenced by the arrangement of buildings and vegetation.

Comparing the integrated solution to the base case simulation, wind speeds remain largely unchanged, as the building positions were not modified; only their heights were adjusted. However, there is a notable shift in wind direction. The addition of vegetation in the upper middle part of the innovation park forces the wind to find alternative pathways to flow through the site.

Reducing building heights has a minor impact on wind behavior, making it easier for air to move across the site. Additionally, the vegetated areas allow for higher wind speeds and smoother flow, contributing to localized cooling, improved ventilation, and heat dissipation.

As shown in Figure 72, the integrated solution and the base case are generally similar in terms of wind speed. However, scenarios involving modified building heights achieve slightly better wind speeds and improved ventilation. In a previous simulation, not only were building heights adjusted, but the distances between them were also increased. This adjustment reduced wind barriers, allowing more air to pass through and resulting in significant differences compared to other scenarios.

While increasing the spacing between buildings may not be practical, the integrated solution focuses solely on reducing building heights. This adjustment moderates wind speed and contributes to cooling and improved airflow throughout the site.

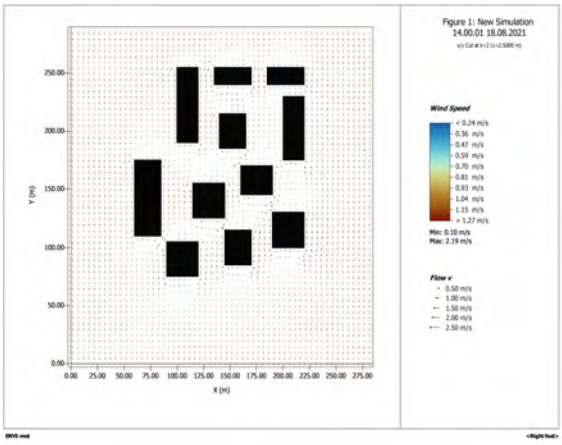

Figure 75: Integrated Solution - Wind Vectors.

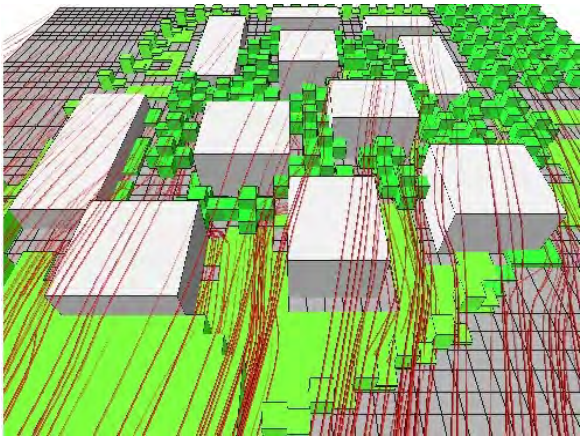

Figure 76: Integrated Solution - 3D Wind Map.

4.2.5 Radiation

The following figures (77, 78, 79, 80) represent respectively direct shortwave (SW) radiation, diffuse shortwave radiation, longwave (LW) radiation from the upper hemispheres and longwave radiation from the lower hemispheres.

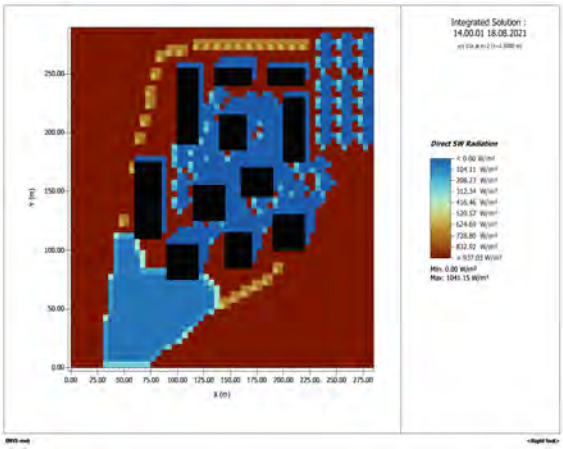

Figure 77: Integrated Solution - Direct SW Radiation.

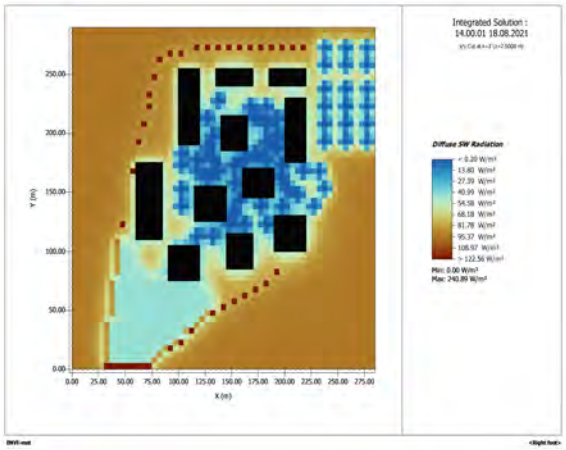

Figure 78: Integrated Solution - Diffuse SW Radiation.

As shown in Figure 77, direct shortwave radiation values range from 0.00 W/m^2 to a maximum of 1041.15 W/m^2. Compared to the base case simulation, significant differences are observed primarily due to vegetation. However, the direct radiation remains largely unchanged in the vegetation microclimate model. In the integrated model, there is a notable reduction in direct shortwave radiation across the entire site, particularly over the parking area, due to the shading effect of trees.

For diffuse shortwave radiation, represented in Figure 78, values range from 0.00 W/m^2 to 240.09 W/m^2. In areas with dense vegetation, less radiation is absorbed and therefore less is diffused. The dense canopies block more sunlight, reducing both direct radiation and diffusion beneath the trees. In contrast, lighter and more spaced-out foliage, such as that of hazel trees, facilitates better diffusion of solar light throughout the site.

The longwave radiation emitted from the upper hemisphere, as illustrated in Figure 79, ranges from 413.09 W/m^2 to 548.35 W/m^2. Unlike shortwave radiation, vegetation absorbs and re-emits more heat than the ground. This is due to vegetation's capacity to absorb thermal energy and radiate it back into the atmosphere.

For the longwave radiation emitted from the lower hemisphere shown in Figure 80, values range from 441.87 W/m^2 to 664.57 W/m^2. In this case, the ground absorbs and re-emits more heat than vegetation. Notably, for both upper and lower hemisphere emissions, the fountains maintain a consistent radiation value of approximately 442 W/m^2, unaffected by surrounding conditions.

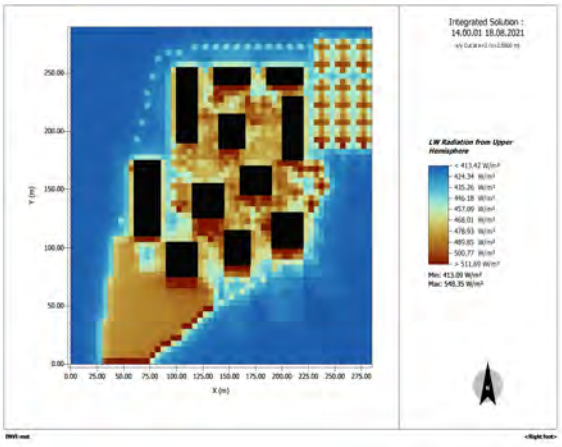

Figure 79: Integrated Solution - LW Radiation Upper Hemisphere.

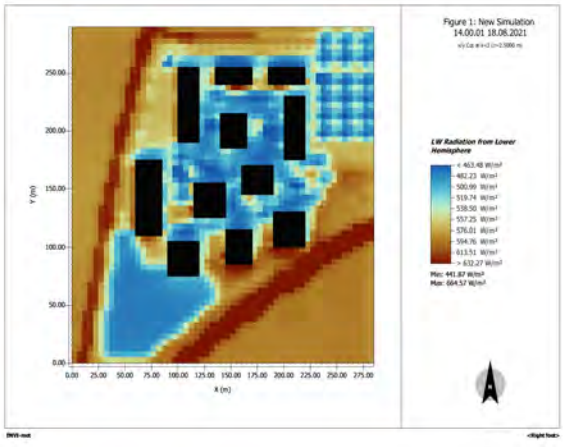

Figure 80: Integrated Solution - LW Radiation Lower Hemisphere.

4.3 Thermal Comfort

Figure 81 illustrates the range of UTCI temperatures after implementing the integrated solution, with values varying from "below 42°C" to "above 50°C." The analysis shows a significant reduction in UTCI values in shaded areas and around the fountains. This indicates that vegetation plays a vital role in enhancing thermal comfort by mitigating direct radiation.

Figure 82 categorizes UTCI values into three thermal stress levels, highlighting notable improvements compared to the base case. The presence of vegetation and water features across the innovation park significantly expands areas with moderate thermal stress (36°C to 42°C). In the base case, this category was limited to zones adjacent to buildings, primarily influenced by shading. In the integrated solution, moderate stress is distributed more evenly due to tree shading and fountain cooling effects. However, areas next to buildings, particularly on their north faces, have reduced moderate-stress zones due to lower building heights.

Strong thermal stress (42°C to 48°C) is observed in regions dominated by grass without dense tree coverage (e.g., field maples), areas without any tree shading (notably parking areas), and near the north faces of buildings. While fountains paired with hazelnut trees improve conditions, they are insufficient to shift these areas into the moderate-stress category. Nonetheless, Figure 81 shows localized improvements in thermal comfort.

Very strong thermal stress (48°C to 60°C) persists in open areas without shade. Hazelnut trees alone cannot sufficiently reduce stress levels in these zones. While replacing the parking ground with light concrete pavement has optimized emissivity and reflectance, leading to reduced surface temperatures, thermal stress remains in the very strong category. Improvements are visible, with UTCI values in the parking area ranging between 46°C and 50°C. This progress results from a combination of tree shading and modified ground materials, although some zones, such as the top-left building's north face, show no real improvement.

The integrated solution demonstrates a clear reduction in UTCI values in shaded areas and around fountains, emphasizing vegetation's critical role in mitigating direct radiation and providing localized cooling. While moderate thermal stress levels have been expanded across the site due to strategic tree placement and fountain usage, areas with insufficient tree coverage remain hotspots for higher thermal stress. Collaborative efforts between shading elements and optimized ground materials show promise but require further refinement for broader and more consistent thermal comfort improvements.

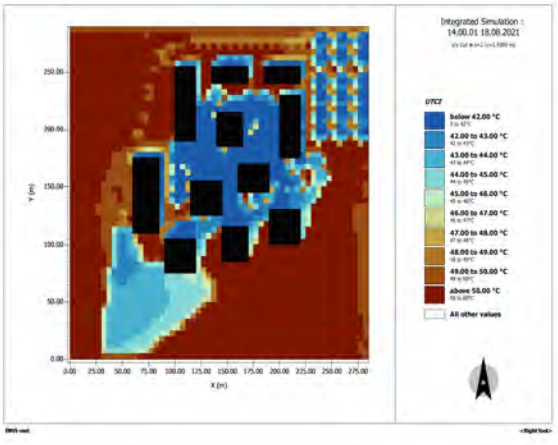

Figure 81: Integrated Solution - UTCI.

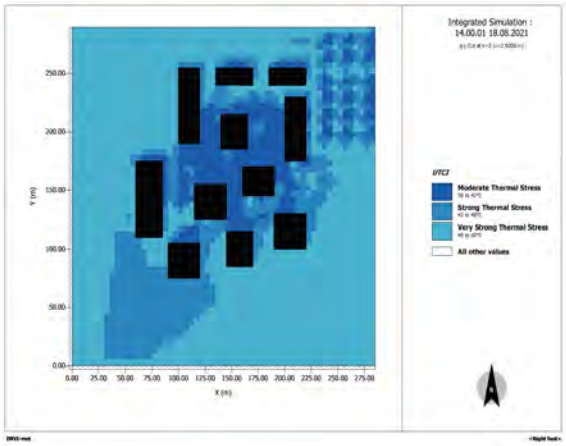

Figure 82: Integrated Solution - Thermal Stress.

5 Conclusion

This microclimatic project at the Innovation park highlights integrated strategies for mitigating the effects of urban heat islands and improving thermal comfort. Based on detailed simulations, it proposes a final solution combining vegetation, ground features, building adjustments and aquatic installations to optimize the site's microclimate.

The mitigation strategy is based on several axes. Firstly, the planting of various types of vegetation, including maples, hazelnuts and grass, provides effective shade, reduces temperatures through evapotranspiration, and increases relative humidity. Secondly, the flooring design favors reflective, permeable or low thermal conductivity materials, such as yellow brick, granite, concrete pavement light or sandy floor. In addition, the introduction of strategically positioned fountains provides localized cooling, particularly in sensitive areas such as car parks. Finally, reducing the height of buildings and installing green roofs improves ventilation, reduces heat absorption and provides natural thermal insulation.

The results of the simulations highlight a number of benefits. There was a significant reduction in surface and air temperatures, of up to 4°C in the shaded areas close to the fountains. Relative humidity increased by up to 15% in the planted areas, making breathing and heating more comfortable. These measures have also led to an extension of moderate heat stress zones (36-42°C), while high heat stress zones ($>$ 48°C) are now limited to areas without plant cover, making vegetation the most important factor in optimizing thermal comfort due to their shaded areas. In addition, the use of permeable and reflective floors has stabilized temperatures and reduced heat build-up, while fountains have improved thermal comfort in critical areas such as car parks.

In conclusion, this project demonstrates that the harmonious interaction between vegetation, materials, water features and buildings can transform the microclimate of a site and reduce the impact of urban heat islands. These interventions offer a pragmatic approach to designing resilient, comfortable and sustainable urban environments in the face of growing climate challenges.

References

[1] ETH Zürich, *Strategies for Cooling Singapore*, Lea A. Ruefenacht & Juan Angel Acero, ETH Library : Zürich, 2017.

6 Appendices

6.1 Site analysis

Group # 2

* no urban canyon formation there

Location	Natural elements	Ground cover material	Surrounding building material	Surrounding building height	Anthropogenic heat source	Aspect ratio	Sky view factor	Shading sources
A	some trees, bushes, plant pots	tar, gravel	Concrete, metal, glass, brick	13 m	cars, people, bus	not relevant, because of parking, few buildings *	~ 1	buildings
B	grass, bushes, trees	tar, little bit of grass	Concrete, metal, glass, brick	13 m	people, cars	w = 15 m ↳ $\lambda_s = \frac{18}{15}$ = 1.2	0.85	buildings
C	bushes, trees	tar, little bit of gravel and grass	Concrete, metal, glass, brick	14 m	people, cars	not relevant *	0.9	bushes, trees, building
D	bushes, trees, grass	gravel, grass	Concrete, metal, glass, brick	22 m	people	not relevant *	0.95	high bushes, big tree
E	small bushes, trees, grass	grass, concrete	Concrete, metal, glass, brick	22 m	people	w = 30 m ↳ $\lambda_s = \frac{18}{30}$ = 0.6	0.75	trees, building
F	small bushes, trees, grass	grass, gravel, soil	Concrete, metal, glass, brick	22 m	people	w = 40 m ↳ $\lambda_s = \frac{18}{40}$ = 0.45	1	trees, building
G	grass, bushes, one tree	grass, concrete, gravel	Concrete, metal, glass, brick	22 m	people	not relevant *	1	tree, building

Figure 83: Site Visit Guide.

.

6.2 Ground-environment interactions

Figure 84: Turfstone.